

The response of calcareous nanoplankton to Oceanic Anoxic Events: The Italian pelagic record

Elisabetta ERBA, Cinzia BOTTINI, Giulia FAUCHER, Gabriele GAMBACORTA & Stefano VISENTIN

- E. Erba, Università degli Studi di Milano, Dipartimento di Scienze della Terra “Ardito Desio”, Via Mangiagalli 34, I-20133 Milano, Italy; elisabetta.erba@unimi.it
C. Bottini, Università degli Studi di Milano, Dipartimento di Scienze della Terra “Ardito Desio”, Via Mangiagalli 34, I-20133 Milano, Italy; cinzia.bottini@unimi.it
G. Faucher, Università degli Studi di Milano, Dipartimento di Scienze della Terra “Ardito Desio”, Via Mangiagalli 34, I-20133 Milano, Italy; giulia.faucher@unimi.it
G. Gambacorta, Università degli Studi di Milano, Dipartimento di Scienze della Terra “Ardito Desio”, Via Mangiagalli 34, I-20133 Milano, Italy; gabriele.gambacorta@guest.unimi.it
S. Visentin, Università degli Studi di Milano, Dipartimento di Scienze della Terra “Ardito Desio”, Via Mangiagalli 34, I-20133 Milano, Italy; stefano.visentin@unimi.it

KEYWORDS - Global anoxia, calcareous nannofossils, palaeoecology, Italian pelagic sections.

ABSTRACT - Earth history is punctuated by phases of extreme global stress of concurrent warming, ocean fertilisation and acidification that impacted biologic diversity and function. Under excess CO₂ and greenhouse conditions, the Mesozoic deep ocean became temporarily depleted of oxygen, promoting the accumulation of massive amounts of organic matter during Oceanic Anoxic Events (OAEs). Although global anoxia and enhanced organic matter burial are the most striking and intriguing palaeoceanographic phenomena, OAEs can be studied also to decipher the oceanic ecosystem response to CO₂ pulses. In Jurassic and Cretaceous oceans, calcareous nanoplankton were already common from coastal to open oceanic settings and of enough abundance and diversity to produce calcareous oozes. Indeed, Jurassic and Cretaceous pelagic micrites mainly consist of coccoliths and nannoliths, in addition to variable amounts of diagenetic carbonate. Therefore, pelagic limestones are ideal for epitomising variations in abundance and composition of calcareous phytoplankton at large scale to understand their response to global change.

Italian pelagic successions are a reference for the Tethys Ocean and, in general, for low to middle latitudes. We consider herein well-dated sections with quantitative nannofossil data across OAEs to synthesise changes in abundance of the dominant, micrite-forming, nannofossil taxa and species-specific variations in size to trace the response of calcareous nanoplankton as expressed by biocalcification across the early Toarcian T-OAE, late Valanginian Weissert-OAE, early Aptian OAE1a and latest Cenomanian OAE2. In general, a major decrease in nannofossil abundance is recorded for the highly calcified dominant forms, evidenced by the “Schizosphaerella crisis”, the “nannoconid decline” and the “nannoconid crisis” during the T-OAE, Weissert-OAE and OAE1a, respectively. An even more dramatic drop in coccolith/nannolith abundance characterises OAE2, with a nanoplankton biocalcification “blackout” through the Bonarelli Level in Italian sections. Despite these abundance crises, calcareous nannofloras recovered soon after the paleoenvironmental perturbation terminated, although the return to pre-OAE conditions occurred rather slowly and assemblage composition was renewed across the event. Species-specific changes in size were detected for Schizosphaerella across the T-OAE and for Biscutum constans (Górka, 1957) in the intervals of maximum perturbation within OAE1a and OAE2. Size of Nannoconus steimannii Kamptner, 1931, conversely, does not show variations across the Weissert-OAE and OAE1a. The T-OAE and OAE1a were preceded and accompanied by a few million-year-long origination phase, indicating the calcareous nanoplankton ability to positively respond to and overcome stressing oceanic conditions, as further evidenced by absence of extinctions. Calcareous nanoplankton reacted differently during the Weissert-OAE and OAE2 as the Valanginian “nannoconid decline” is gradual and followed by a symmetric increase in abundance, while the late Cenomanian nannofossil drop in abundance was as sudden as its recovery. In both cases, extinctions are paralleled by entry of new taxa, at a slower rate across the Weissert-OAE and at faster rates in the case of OAE2. The influence of palaeoenvironmental stress on calcareous nannofloral abundance and composition during the early Toarcian T-OAE, late Valanginian Weissert-OAE, early Aptian OAE1a and latest Cenomanian OAE2, are clearly recorded in Italian pelagic sections and at supra-regional to global scale. However, the effects on nanoplankton evolution, if any, was differentiated and resulted in overall originations. Calcareous nannofossil patterns underline the resilience of this phytoplankton group during OAE perturbations.

RIASSUNTO - [La risposta del nanoplancton calcareo agli Eventi Anossici Oceanici: il record pelagico in Italia] - La storia della Terra è punteggiata da eventi di stress globale estremo evidenziato da riscaldamento, fertilizzazione e acidificazione oceanica che hanno influito sulla diversità e sul funzionamento del biota marino. In condizioni di eccesso di CO₂ e di clima a effetto serra, durante il Mesozoico i fondali marini hanno sperimentato temporanea anossia e accumulo di materia organica durante eventi anossici oceanici (OAE). Sebbene l'anossia globale e il seppellimento di grandi quantità di carbonio organico siano i fenomeni paleoceanografici più intriganti, gli OAE possono essere studiati anche per decifrare la risposta dell'ecosistema oceanico a perturbazioni globali. Negli oceani del Giurassico e Cretacico, il nanoplancton calcareo era già diffuso dalle zone costiere all'oceano aperto, in sufficiente abbondanza e diversità per produrre sedimenti biogenici calcarei. Infatti, le micriti pelagiche del Giurassico e del Cretacico consistono principalmente di coccoliti e nannoliti, oltre a quantità variabili di carbonato diagenetico. Pertanto, i calcari pelagici sono ideali per quantificare le variazioni di abbondanza e composizione del fitoplancton calcareo e, di conseguenza, dei produttori primari per comprenderne la risposta ai cambiamenti globali.

Le successioni pelagiche italiane sono considerate di riferimento per l'Oceano della Tetide e, in generale, per le basse-medie latitudini. In questo lavoro, abbiamo considerato sezioni stratigrafiche ben datate e con dati quantitativi delle associazioni a nannofossili calcarei, per sintetizzare i cambiamenti in abbondanza dei taxa dominanti e le variazioni dimensionali di alcune specie al fine di tracciare la risposta del nanoplancton calcareo tramite la biocalcificazione durante il T-OAE del Toarciano inferiore, il Weissert-OAE del Valanginiano superiore, l'OAE1a dell'Aptiano inferiore e l'OAE2 del Cenomaniano sommitale. In generale, si registra una drastica diminuzione dell'abbondanza dei nannofossili, soprattutto per le forme dominanti altamente calcificate, come evidenziato dalla “crisi di Schizosphaerella”, dal “declino dei nannoconidi” e dalla “crisi dei nannoconidi” durante i T-OAE, Weissert-OAE e OAE1a, rispettivamente. Una riduzione ancora più drammatica dell'abbondanza di coccoliti/nannoliti caratterizza l'OAE2, con un “blackout” della biocalcificazione del nanoplancton durante

la deposizione del Livello Bonarelli nelle sezioni italiane. Nonostante queste crisi di abbondanza, le nannoflore calcaree si sono ristabilite subito dopo la fine della perturbazione paleoambientale, sebbene il ritorno a condizioni pre-OAE sia avvenuto piuttosto lentamente e le associazioni abbiano raggiunto una composizione diversa. Sono stati rilevati cambiamenti delle dimensioni di *Schizosphaerella* attraverso il T-OAE e di *Biscutum constans* (Górka, 1957) negli intervalli di massima perturbazione all'interno degli OAE1a e OAE2. Le dimensioni di *Nannoconus steimannii* Kamptner, 1931, al contrario, non mostrano variazioni durante il Weissert-OAE e l'OAE1a. Il T-OAE e l'OAE1a sono stati preceduti e accompagnati da una fase di speciazione del nannoplancton, durata alcuni milioni di anni, che indica la capacità del fitoplancton calcareo a rispondere positivamente superando condizioni oceaniche stressanti, come evidenziato anche dall'assenza di estinzioni. Il nannoplancton calcareo ha reagito in modo diverso durante il Weissert-OAE e l'OAE2 poiché il "declino dei nannoconidi" del Valanginiano è graduale e seguito da un altrettanto graduale aumento dell'abbondanza, mentre la riduzione dei nannofossili nel Cenomaniano sommitale è stata repentina come il suo recupero. In entrambi i casi, si sono verificate alcune estinzioni ma contemporaneamente anche la speciazione di nuovi taxa, a un ritmo più lento attraverso il Weissert-OAE e a tassi più rapidi nel caso dell'OAE2.

Mentre l'influenza dello stress paleoambientale sull'abbondanza e composizione delle nannoflore calcaree durante il T-OAE, il Weissert-OAE, l'OAE1a e l'OAE2 è chiaramente registrata nelle sezioni pelagiche italiane e spesso su scala sopra-regionale fino a globale, l'influenza degli OAE sull'evoluzione del nannoplancton, se causale, è stata differenziata e ha generalmente indotto delle speciazioni. Le variazioni riscontrate nelle associazioni a nannofossili calcarei sottolineano la resilienza di questo gruppo di fitoplancton durante le perturbazioni ambientali associate agli OAE.

INTRODUCTION

The early phase of the Deep Sea Drilling Project provided evidence of extensive occurrence of Cretaceous black shales from previously unsampled oceanic basins. As on-land, stratigraphies of pelagic successions showed that organic carbon-rich lithologies are confined to specific geologically short intervals (0.5 to 2 million years) suggesting a global rather than local to regional oxygen-depletion of bottom waters.

The term "Oceanic Anoxic Event" (OAE) was coined by Schlanger & Jenkyns (1976) after the recovery of mid-Cretaceous black shales at sites drilled in the Pacific Ocean. Such lithologic units were recognised as equivalent and coeval of well-known lithostratigraphic markers previously described in the Tethys and Atlantic Oceans. The term OAE was originally defined to signify time intervals during which black shale deposition was prevalent at a global scale. The original definition was, therefore, based on lithologic criteria and applied to two time intervals, namely the Aptian-Albian (OAE1) and the Cenomanian-Turonian (OAE2). Later investigations on land and in the oceans pointed out the occurrence of the Coniacian-Santonian OAE3 (Arthur & Schlanger, 1979; Jenkyns, 1980) and of the Toarcian OAE (Jenkyns, 1985, 1988). Based on integrated and higher resolution stratigraphy of the sedimentary record of organic-rich black shales, Arthur et al. (1990) subdivided OAE1 into discrete events OAE1a, OAE1b, OAE1c and OAE1d, still using the sedimentary record of organic C-rich black shales.

The most spectacular sedimentary expression of the early Aptian and latest Cenomanian events are the Livello Selli and Livello Bonarelli, respectively. For both the type area is the Umbria-Marche Basin (central Italy), where a continuous pelagic succession deposited in the Jurassic to

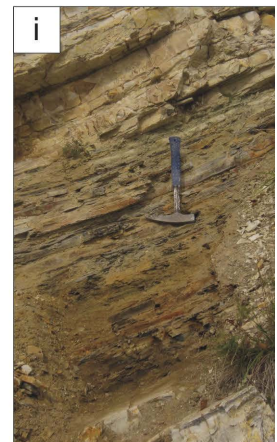
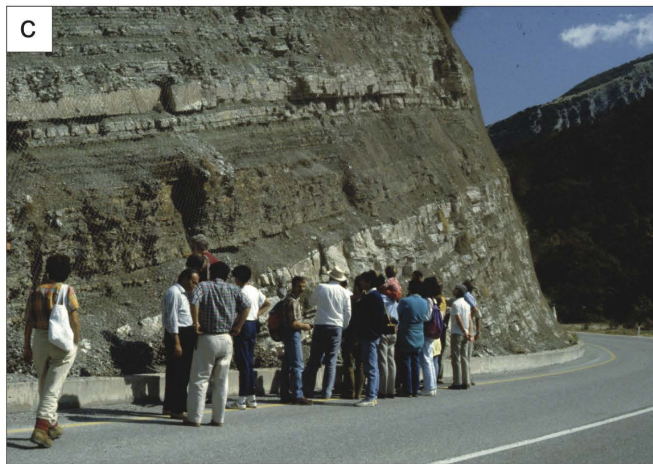
Paleogene interval. The first event that was recognised and the most studied one is the Bonarelli Level, named after its discoverer Guido Bonarelli. In fact, in 1891 Bonarelli described "uno strato di scisto nero bituminoso" (a level of black organic-rich shale), about 1 metre thick, in the uppermost part of the Scaglia Bianca in the region of Gubbio, close to the Cenomanian/Turonian boundary (Bonarelli, 1891) (Fig. 1).

At the beginning of the XX century, Dal Piaz (1907) described Toarcian organic-rich facies in pelagic Jurassic successions of the Alpi Feltrine in the Southern Alps, similarly to other occurrences in Germany and Switzerland (Posidonienschiefer), England (Jet Rock and Bituminous Shales) and France (Schistes Carton). Dal Piaz's perception of black shales as geological archives of major environmental changes was by far innovative and a precursor of modern palaeoceanography. A few decades later Gaetani & Poliani (1978) described a lower Toarcian black shale interval, named "Livello a Pesci" (Fish Level), in the pelagic succession of the Lombardy Basin (Fig. 1). In the 80s, Jenkyns (1985, 1988) labelled these black shale intervals as the Toarcian OAE (T-OAE).

The identification of the Livello Selli is much younger (Coccioni et al., 1987) and, again, was based on the occurrence of a 1-3 m thick marker bed described as a "livello radiolaritico-bituminoso-ittiolitico" (a black shale interval enriched in radiolarians, fish remains and organic matter) in the lowermost part of the Marne a Fucoidi Formation through the Umbria-Marche Basin (Fig. 1).

With the rapid development of chemostratigraphy, and specifically of C and O stable isotopic investigations, it became clear that the T-OAE, OAE1a and OAE2 are associated with negative and positive anomalies of carbon-isotope curves obtained from sedimentary carbonate and/or organic matter, which record major perturbations of

Fig. 1 - a) "Livello a Pesci", deposited during the T-OAE, at the Colle di Sogno section (n. 3 in Fig. 3 - Lombardy Basin, northwestern Italy). b) "Livello a Pesci" in the Sogno Core compared to the equivalent outcropping lithostratigraphic interval (n. 3 in Fig. 3 - Lombardy Basin, northwestern Italy). c) Selli Level, deposited during the OAE1a, at the Apecchiese section. The laterally equivalent interval was cored nearby in the Piobbico Core (n. 17 in Fig. 3 - Umbria-Marche Basin, central Italy). d) Selli Level equivalent recovered with the Cismon APTICORE placed next to the same outcropping lithostratigraphic interval (n. 11 and 12 in Fig. 3 - Belluno Basin, northeastern Italy). e) The Weissert-OAE interval (bounded by the two yellow dashed lines) at Polaveno (n. 6 in Fig. 3 - Lombardy Basin, northwestern Italy). f) The middle Cenomanian to lower Turonian succession at Furlo (n. 15 in Fig. 3 - Umbria-Marche Basin, central Italy) with the black shales of the Livello Bonarelli deposited during OAE2. g) Close up view of Livello Bonarelli in the Contessa outcrop (n. 24 in Fig. 3 - Umbria-Marche Basin, central Italy). h) Close up view of Livello Bonarelli in the Bottaccione Gorge section (n. 22 in Fig. 3 - Umbria-Marche Basin, central Italy). i) Close up view of Livello Bonarelli in the Monte Petrano section (n. 18 in Fig. 3 - Umbria-Marche Basin, central Italy).



the global carbon cycle (Jenkyns, 2010). The original definition of OAEs (Schlanger & Jenkyns, 1976) has become somehow misleading for various reasons: 1) anoxia is rarely reached; 2) black shale intervals were proved to be diachronous in many cases; 3) fully oxic continental and shallow marine successions also record the global C cycle anomalies; 4) anomalies are of long to short duration.

High-resolution integrated stratigraphy of marine and terrestrial records has produced a solid time framework for OAEs (Robinson et al., 2017), and $\delta^{13}\text{C}$ chemostratigraphy has grown as the prominent tool for identifying, characterising and correlating OAEs (e.g., Erba, 2004; Tsikos et al., 2004; Weissert & Erba, 2004; Jenkyns, 2010). A typical example is the discrete C isotope excursion of late Valanginian age identified in the Maiolica Formation of the Southern Alps (Weissert, 1989; Lini et al., 1992), which is not accompanied by a black marker bed (Fig. 1). Such an anomaly was constrained by bio-magnetostratigraphy (Channell et al., 1993) and used by Erba et al. (2004) to formalise the Valanginian event as the “Weissert OAE”. Global anoxia has not been documented, but discrete black shale levels enriched in organic matter are described from the Tethys and Pacific Oceans in the early phase of the Weissert-OAE (Erba et al., 2004).

In the past four decades OAEs have been recognised in oceanic and terrestrial sequences, highlighting local variations in depositional conditions, types and degrees of diagenesis, and preservation of organic matter. As summarised by Jenkyns (2010), equivalents of the Bonarelli, Selli, Weissert and Toarcian events have been recognised in a variety of sedimentary basins, and a number of geochemical anomalies have been detected in addition to C-isotope excursions. Yet, a lively debate about causes and consequences of OAEs and their influence on biota continues to involve experts from various disciplines within geosciences. The original hypotheses of Schlanger & Jenkyns (1976) are still discussed to discern and discriminate the role of productivity from that of organic matter preservation under anoxic conditions. Pelagic successions containing OAEs are crucial to understand the biotic variations in marine planktonic communities associated with such global perturbations of the ocean/atmosphere system. In marine ecosystems coccolithophores are part of phytoplankton responsible for primary productivity, energy transfer to higher trophic levels, export of biogenic particles to the seafloors and exchanges between the surface ocean and the atmosphere. The term calcareous nannoplankton was originally introduced by Lohman (1902) for planktonic organisms smaller than 63 μm and is now used for golden-brown algae coccolithophores (phylum Haptophyta) secreting tiny calcite crystals to build coccoliths and ultimately coccospheres. The global occurrence of calcareous nannoplankton and their biomineralisation make these phytoplanktonic algae a very effective producer of calcite on Earth. Calcareous nannofossils include the fossil remains of coccolithophores, namely coccoliths and coccospheres as well as associated nannoliths often of unknown biological affinity.

In Jurassic and Cretaceous oceans, calcareous nannoplankton were already the most efficient rock-forming group (e.g., Erba, 2006). Indeed, Jurassic and

Cretaceous pelagic micrites mainly consist of coccoliths and nannoliths, in addition to variable amounts of diagenetic calcite. Consequently, pelagic carbonates offer the opportunity of characterising variations in abundance and composition of calcareous nannofloras across OAEs to quantify their resilience to extreme conditions.

Italian pelagic successions represent excellent records of the Tethys Ocean (Figs 1-2) and, in fact, have been studied since a long time. The first documentations of nannofossil-rich limestones were based on scanning electron microscope investigations of Maiolica and Scaglia limestones (Farinacci, 1964). These pioneering studies unequivocally demonstrated the rock-forming role of calcareous nannoplankton as further discussed by Noël & Busson (1990) also for Jurassic pelagic successions of the Tethys. Indeed, it became clear that *Schizosphaerella* and *Nannoconus* can reach high abundances in pelagic and hemipelagic carbonates of Jurassic and Cretaceous age. The name “nannoconite” was proposed for *Nannoconus*-limestone (Bréhéret, 1983) and quantitative studies conclusively showed that Lower Cretaceous Maiolica limestones are nannoconites (Erba, 1994; Erba & Tremolada, 2004). Similarly, *Schizosphaerella* can be so abundant (e.g., Kälin & Bernoulli, 1984; Claps et al., 1995; Mattioli, 1997; Erba, 2004; Casellato & Erba, 2015; Peti & Tibault, 2017) as to produce a “schizosphaerellite”.

Quantitative studies of Cretaceous pelagic successions, comprising OAEs, reveal major shifts in the biogenic component: from carbonate-dominated to siliceous- and organic matter-dominated (Premoli Silva et al., 1999; Leckie et al., 2002; Erba, 2004). Usually, radiolarian and organic-walled micro-organisms become overwhelming in the black shales representing OAEs, while calcareous nannofossils are abundant below and above. The nannofossil record, in fact, traces major decreases in abundances across the perturbation, especially of the dominant forms that usually show incomplete recovery after termination of OAEs (Erba, 2004).

Erba (2004) reviewed changes in calcareous nannofossil assemblages across the T-OAE, OAE1a and OAE2 and proposed palaeoceanographic and palaeoecologic dynamics. In this work, we focus on calcareous nannofossil changes across OAEs recorded in pelagic Italian successions that are, still, reference records of global changes at low to middle latitudes. Our synthesis regards only well-dated sections with quantitative nannofossil data and $\delta^{13}\text{C}$ chemostratigraphy for the T-OAE, Weissert-OAE, OAE1a and OAE2. In particular, for each OAE we will highlight changes in abundance of the dominant (micrite-forming) nannofossil taxa and species-specific variations in size to trace the response of calcareous nannoplankton as expressed by their biocalcified remains.

MATERIAL AND METHODS

A geographical map showing the location of the sections considered for this work is given in Fig. 3, while Fig. 2 shows the palaeogeography of the Tethyan area during the Jurassic-Cretaceous interval. Considered sections mostly lie in the Southern Alps (sections 1 to 14) and the Umbria-Marche Basin (sections 15 to 27),

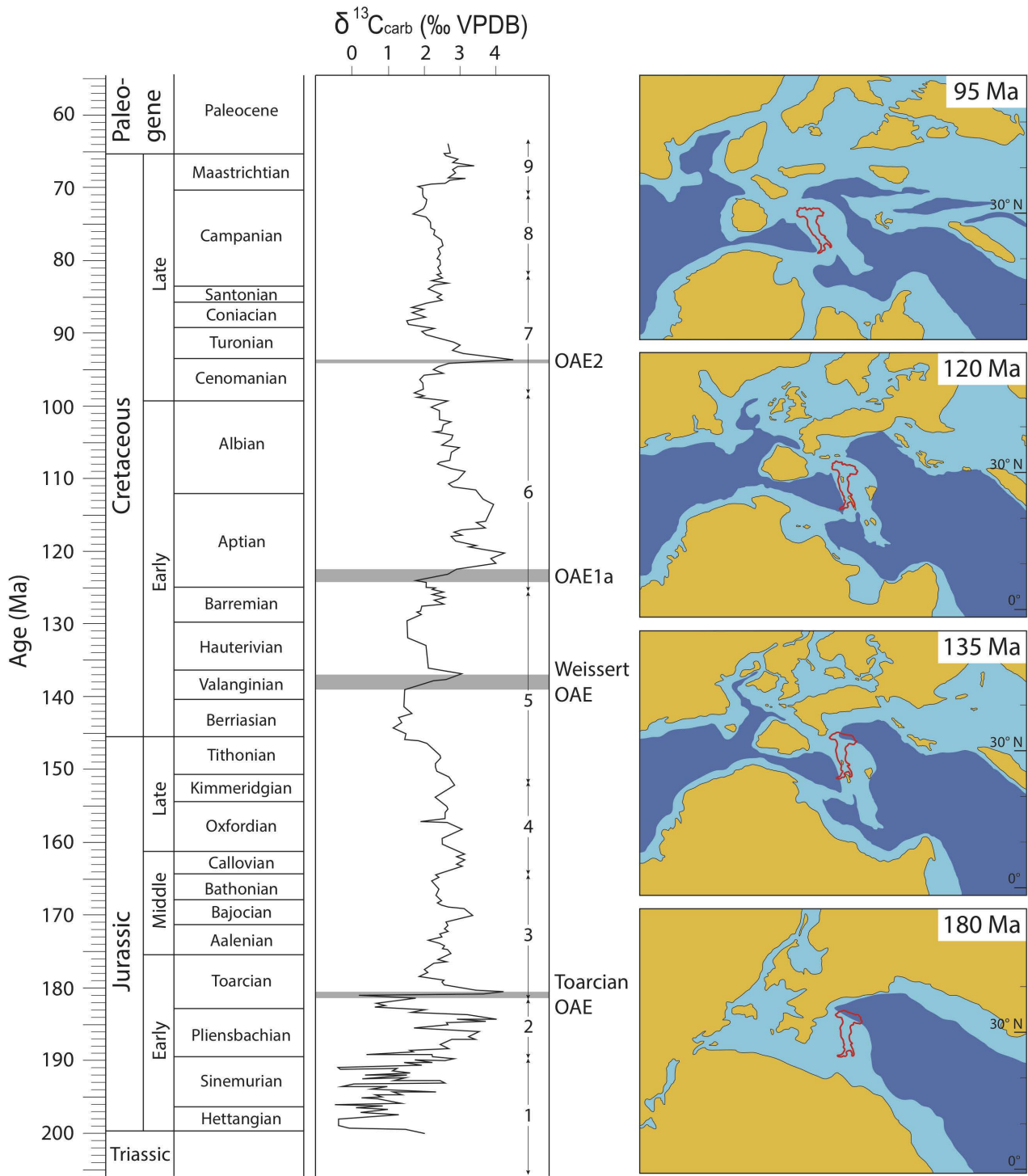


Fig. 2 - Bulk carbonate carbon isotope ($\delta^{13}\text{C}_{\text{carb}}$) stratigraphy of the Jurassic and Cretaceous (modified after Robinson et al., 2017). The stratigraphic position of T-OAE, Weissert-OAE, OAE1a and OAE2 are reported as grey bands. Carbon-isotope data from: (1) Van de Schootbrugge et al. (2005); (2) Hesselbo et al. (2000); (3) Morettini et al. (2002); (4) Dromart et al. (2003); (5) Weissert et al. (1998); (6) Erbacher et al. (1996); (7) Jenkyns et al. (1994); (8) Jarvis et al. (2002); and (9) Abramovich et al. (2003). On the right the relative position of Italy at 180 Ma, 135 Ma, 120 Ma and 95 Ma is reported as a red outline on palaeogeographic maps (modified after Scotese, 2014).

but a few key-successions were studied in the Gargano area (section 28), Sicily (sections 29 to 31) and Sardinia (section 32). The sedimentary expression of the T-OAE, Weissert-OAE, OAE1a and OAE2 in Italian key-sections is illustrated in Fig. 1. For this review we considered all the published papers documenting quantitative and

morphometric data for calcareous nannofossils across the T-OAE, Weissert-OAE, OAE1a and OAE2, within a well-defined framework of C-isotope stratigraphy (see Tabs 1-4). The data are summarised in a graphical form by reporting as bars the relative stratigraphic range of each section, separately for nannofossil and $\delta^{13}\text{C}$ data. In

case the same section was described in multiple papers, we synthesised in a single bar the cumulative extent of the data generated for the analysed stratigraphic interval (Tabs 1-4). The presence and extension of hiatuses are also reported. The resulting synthesis figures are intended to help the reader in rapidly identifying the relevant literature and have an overall framework of C-isotope chemostratigraphy applied to Jurassic and Cretaceous OAEs in Italian sections.

As previously discussed, the operational definition of OAEs has partially changed, and various authors based OAE boundaries (onset and termination) on lithostratigraphic or chemostratigraphic data. In most cases biostratigraphy was used to constrain age attribution and possibly identify/confirm hiatuses eliding part of the OAEs. It should also be stressed that in many cases black shales are diachronous, defying the original definition of Schlanger & Jenkyns (1976). The definitions adopted in this paper are as follows:

1. The T-OAE corresponds to the negative excursion in the carbonate and organic carbon isotope profile (Jenkyns, 2010).

2. The Weissert-OAE is based on the $\delta^{13}\text{C}$ curve: its beginning and end are placed at the base of the positive excursion and its climax, respectively (Erba et al., 2004).

3. The early Aptian OAE1a corresponds to the Selli Level. With reference to the $\delta^{13}\text{C}$ chemostratigraphy, it begins with the onset of the sharp negative shift named C3-Ap3, and terminates at the base of the extended positive excursion named C7-Ap7 (Menegatti et al., 1998; Bottini et al., 2015).

4. The definition of the latest Cenomanian OAE2 is based on the $\delta^{13}\text{C}$ curve: its beginning and end are placed at the base of the positive excursion and at its climax, respectively (Tsikos et al., 2004).

As discussed by Jenkyns (2010), the amplitude of the carbon isotope anomaly is usually greater in marine and terrestrial organic matter than in carbonate. However, when bulk $\delta^{13}\text{C}_{\text{carb}}$ chemostratigraphy is considered, absolute values and trends are very comparable in many marine sections, allowing the construction of reference synthesis curves (e.g., Erba, 2004; Weissert & Erba, 2004; Jarvis et al., 2006; Robinson et al., 2017; Bottini & Erba, 2018) (Fig. 3).

As far as Italian sections are concerned, quantitative analyses of nannofossil abundances of Lower Jurassic (T-OAE) and Lower Cretaceous intervals (Weissert-OAE and OAE1a) were performed on ultrathin sections by light polarising microscope at 1250 \times magnification. Thin sections were thinned to an average thickness of 7

ITALIAN PELAGIC SECTIONS WITH NANNOFOSSIL AND CARBON ISOTOPIC DATA FOR T-OAE

n.	Locality	Reference	Nannofossils	$\delta^{13}\text{C}$
1.	Val Ceppelline (Lombardy Basin, northwestern Italy)	Jenkyns & Clayton, 1986		•
3.	Colle di Sogno/Mt. Brughetto (Lombardy basin, northwestern Italy)	Jenkyns & Clayton, 1986 Casellato & Erba, 2015	•	•
8.	Brasa (Lombardy Basin, northwestern Italy)	Cobianchi & Picotti, 2001	•	
14.	Dogna (Belluno Basin, northeastern Italy)	Jenkyns et al., 2001		•
20.	Valdorbina (Umbria-Marche, central Italy)	Jenkyns & Clayton, 1986 Sabatino et al., 2009		• •
21.	Colle d'Orlando (Umbria-Marche, central Italy)	Bucefalo Palliani et al., 1998 Mattioli & Pittet, 2004	• •	
25.	Pozzale (Umbria-Marche, central Italy)	Bucefalo Palliani et al., 1998 Mattioli et al., 2004b Mattioli & Pittet, 2004	• • •	•
26.	Somma (Umbria-Marche, central Italy)	Mattioli & Pittet, 2002 Mattioli et al., 2004a Mattioli et al., 2004b Mattioli et al., 2009	• • • •	• •
27.	Fonte Cerro (Umbria-Marche, central Italy)	Bucefalo Palliani et al., 1998 Mattioli & Pittet, 2004	• •	

Tab. 1 - Compilation of papers documenting quantitative nannofossil and carbon isotope data for the T-OAE interval.



Fig. 3 - Geographic location of the Italian sections with available quantitative and morphometric nannofossil and/or carbon isotope data for the T-OAE, Weissert-OAE, OAE1a and OAE2.

mm in order to have an adequate view of nannofloras, and nannofossil absolute abundances were calculated counting all specimens in 1 mm² (Erba, 1994, 2004; Erba & Tremolada, 2004; Bottini et al., 2015; Casellato & Erba, 2015). For the OAE2 interval, total nannofossil abundances were obtained on simple smear slides: the nannofossil assemblages were quantified by counting at least 300 specimens in each sample using a light polarising microscope at 1250× magnification, and the total abundance was calculated as the average number of nannofossils per field of view (Erba, 2004).

In addition to trends of nannofossil abundances, we report here species-specific changes in size of selected taxa across the T-OAE, Weissert-OAE, OAE1a and OAE2. Particularly, morphometric investigations were applied to capture size fluctuations of: 1) *Schizosphaerella* across the T-OAE; 2) *Nannoconus steinmannii* Kamptner, 1931 across the Weissert-OAE; 3) *N. steinmannii* and *Biscutum constans* (Górka, 1957) across OAE1a; 4) *Biscutum constans* across OAE2. Size measurements were carried out on simple smear slides. Morphometry of *Schizosphaerella* and *B. constans* is based on digital photographs acquired with a camera mounted on a Leitz Laborlux light microscope and using the ImageJ64 software. Morphometric analyses of *N. steinmannii*, instead, were obtained with built-in camera Olympus

DP73 set on the light microscope Leica DM2700P and using the Fiji software (Schindelin et al., 2012).

Schizosphaerella specimens were measured taking into account the maximum diameter of the valve (Fig. 4), similarly to Mattioli & Pittet (2002). Nannoliths of *N. steinmannii* are shaped like an elongated frustum of cone, and measured parameters include the maximum width (base width), the minimum width (top width) and the height (Fig. 4). In addition, the volume of each specimen was calculated. Coccoliths of *B. constans* are elliptical in shape, consequently length and width were measured for individual specimens (Fig. 4).

NANNOFOSSIL ABUNDANCE AND SIZE CHANGES ACROSS OAES

Previous papers documented variations in calcareous nannofloral assemblage composition related to palaeotemperature and palaeofertility fluctuations and nannofossil indices were reconstructed for the intervals prior to, during and after OAES recorded in Italian sections (Erba, 2004; Bottini et al., 2015; Casellato & Erba, 2015; Bottini & Erba, 2018). In this chapter we synthesise and discuss the changes in calcareous nannofossil abundance and coccolith/nannolith size as potential proxies of bioalcalification adjustments under altered oceanic carbonate chemistry. Data are presented in stratigraphic order from the oldest to the youngest OAE.

The Toarcian T-OAE

A total of nine Italian pelagic sections cover the T-OAE (Fig. 5): the Val Ceppelline, Colle di Sogno and Brasa sections in the Lombardy Basin, the Dogna section in the Belluno Basin, the Valdorbia, Colle d'Orlando, Pozzale, Somma and Fonte Cerro sections in the Umbria-Marche Basin. Six out of the nine sections were investigated for carbon isotope chemostratigraphy, while for three sections the identification of the stratigraphic position of the T-OAE was based on biostratigraphy. As summarised in Tab. 1, a limited amount of papers documents the occurrence of the Toarcian C isotopic anomaly in Italian sections. In particular, it is important to stress that for the Val Ceppelline and Colle di Sogno sections nothing was published in recent years, as the only C isotopic data were presented by Jenkyns & Clayton (1986). The Dogna (Jenkyns et al., 2001) and Valdorbia (Sabatino et al., 2009) sections undoubtedly represent to date the best available Italian record, with a high-resolution comparable to

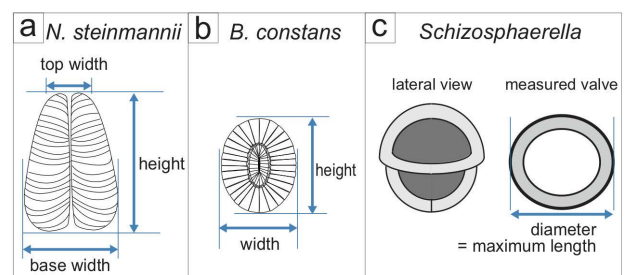


Fig. 4 - Measured parameters of selected nannofossil taxa: a) *Nannoconus steinmannii*; b) *Biscutum constans* and c) *Schizosphaerella*.

ITALIAN PELAGIC SECTIONS WITH NANNOFOSSIL AND CARBON ISOTOPIC DATA FOR WEISSERT-OAE

n.	Locality	Reference	Nannofossils	$\delta^{13}C$
2.	Pusiano (Lombardy Basin, northwestern Italy)	Channell et al., 1993	•	•
4.	Rio Corna (Lombardy Basin, northwestern Italy)	Lini et al., 1992		•
5.	Capriolo (Lombardy Basin, northwestern Italy)	Lini et al., 1992		•
6.	Polaveno (Lombardy Basin, northwestern Italy)	Lini et al., 1992		•
		Bersezio et al., 2002	•	
		Erba & Tremolada, 2004	•	
		This work	•	
9.	Valle Aviana (Trento Plateau, northeastern Italy)	Lini et al., 1992		•
13.	Val del Mis (Belluno Basin, northeastern Italy)	Channell et al., 1993		•
19.	Chiaserna Monte Acuto (Umbria-Marche, central Italy)	Sprovieri et al., 2006		•
32.	S'Ozzastru (Sardinia, Italy)	Bottini et al., 2018		•

Tab. 2 - Compilation of papers documenting quantitative nannofossil and carbon isotope data for the Weissert-OAE interval.

modern standards. We highlight that for the Brasa section in the Lombardy Basin and the Colle d'Orlando and Fonte Cerro sections in the Umbria-Marche Basin, no carbon isotopic data were published.

Quantitative and semiquantitative nannofossil data are available for the Colle di Sogno (Casellato & Erba, 2015), Brasa (Cobianchi & Picotti, 2001), Colle d'Orlando,

Pozzale, Somma and Fonte Cerro sections (Bucefalo Palliani et al., 1998; Mattioli & Pittet, 2004) (Fig. 5). Morphometric analyses of *Schizosphaerella* are available for the Somma section (Mattioli et al., 2004b, 2009) and were obtained for the Sogno Core (this study) drilled at Colle di Sogno. Quantitative analyses of *Schizosphaerella punctulata* Deflandre & Dangeard, 1938 and *Mitrolithus*

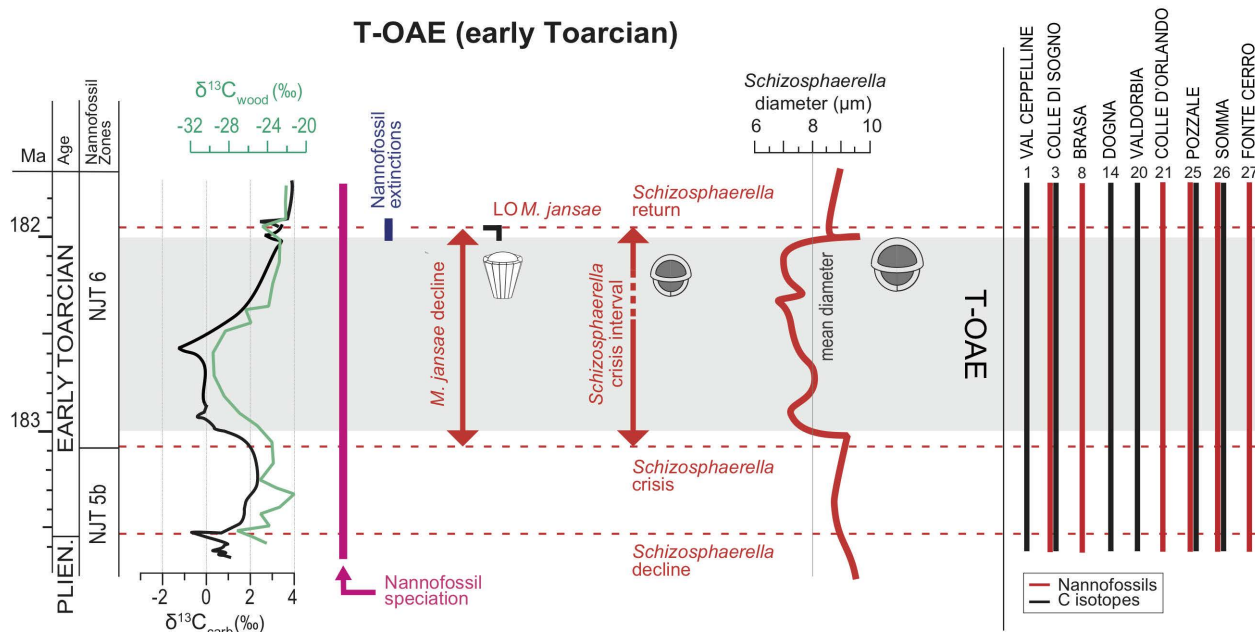


Fig. 5 - On the left: synthesis of calcareous nannofossil changes through the Toarcian-OAE (ca. 183 Ma). Nannofossil origination and extinction intervals are reported as pink and blue bars, respectively. The *Schizosphaerella* and *M. jansae* variations in abundance and the diameter of *Schizosphaerella* (three point moving average of the diameter) are reported (this study). On the right: the stratigraphic extent of published (semi)quantitative nannofossil data (red bar) and available inorganic and/or organic stable carbon isotope record (black bar) is reported for each section. Section numbering as in Fig. 3. The T-OAE is indicated with a grey band. The time scale is after Gradstein et al. (2012). Carbon isotope curve is modified after Hesselbo et al. (2007), Peniche section (Portugal).

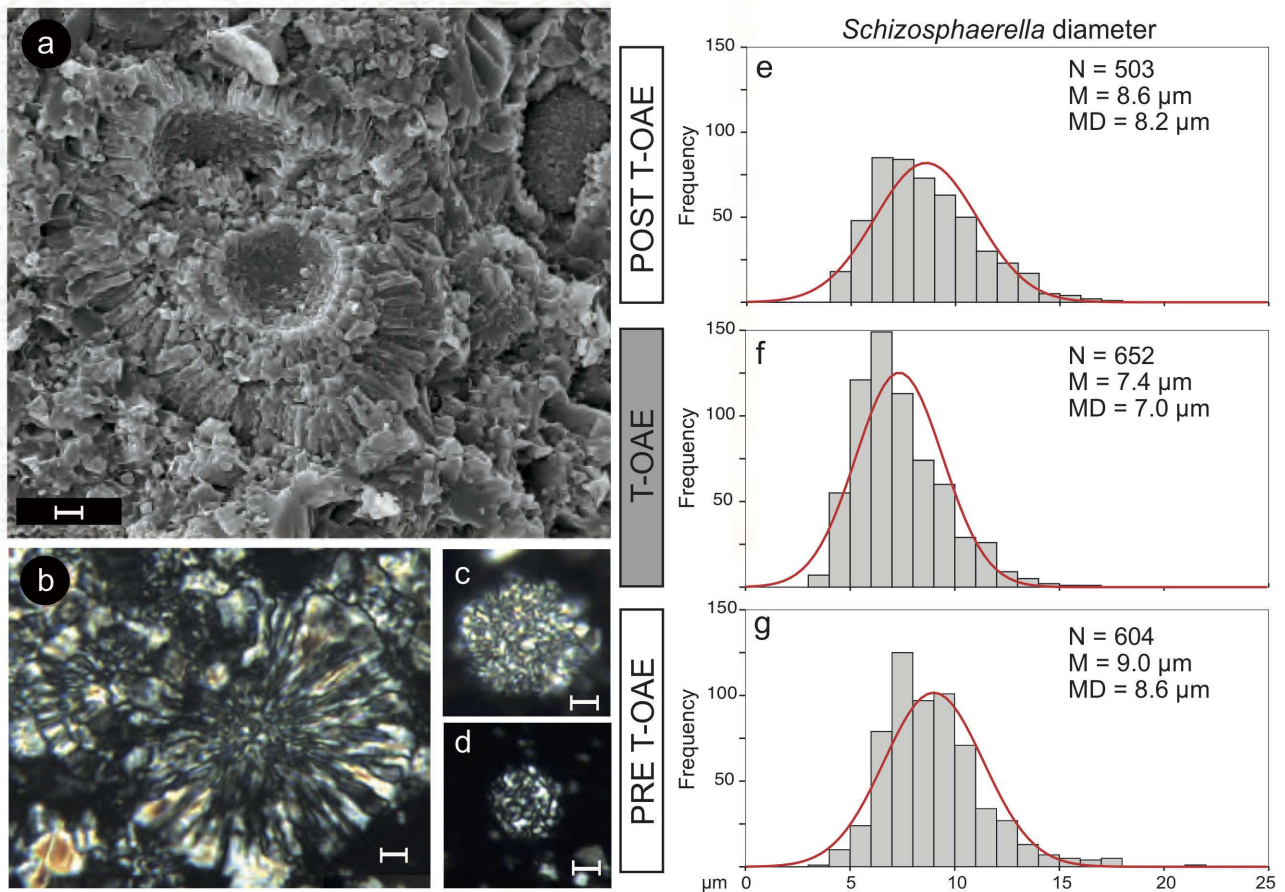


Fig. 6 - a-d) Images of *Schizosphaerella* from the Colle di Sogno section (after Casellato & Erba, 2015); scale bar = 2µm. a) Scanning electron microscope of a *Schizosphaerella*-micrite from the uppermost Domaro Limestone. b) Light polarising microscope image of a cluster of *Schizosphaerella* from the uppermost Domaro Limestone. c) Light polarising microscope image of *S. punctulata* from the topmost Domaro Limestone. d) Light polarising microscope image of "small *S. punctulata*" from the lowermost Sogno Formation. e-g) Results of mixture analysis of samples with estimated mean diameter (M), median diameter (MD) and number of specimens analysed (N) subdivided in three intervals: e) pre- T-OAE, f) T-OAE and g) post - T-OAE, analysed in the Colle di Sogno section and Sogno Core (this study).

jansae (Wiegand, 1984) identified changes in abundance of these taxa across the T-OAE (Casellato & Erba, 2015). After a period of stability and oligotrophy dominated by the rock-forming deep-dwellers (Fig. 5), enhanced nutrient availability under increased run-off, possibly induced the "*Schizosphaerella* decline" close to the Pliensbachian/Toarcian boundary, also accompanied by a marked decrease in abundance of *M. jansae* and an increase in abundance of *Biscutum* and *Lotharingius* (Casellato & Erba, 2015). Just before the onset of T-OAE, a further drop in abundance is shown by both *Schizosphaerella* and *M. jansae*, with the exclusion of "encrusted *S. punctulata*" and the survival of "thin *M. jansae*" (Casellato & Erba, 2015). In the Fish Level both *S. punctulata* and *M. jansae* drop in abundance while small coccoliths show an increase in abundance that, however, contributed very little to calcite production, justifying the low carbonate content of the T-OAE black shales at Colle di Sogno (Casellato & Erba, 2015). In the interval above the Fish Level, nannofossils are mostly represented by small taxa with some contribution by *S. punctulata*, while *M. jansae* barely survived the palaeoenvironmental stress and disappeared soon after the T-OAE termination (Fig. 5). Indeed, after the end of anoxia, palaeoceanographic conditions in the

photic zone resumed gradually to a pre-perturbation state, as suggested by calcareous nannofloral assemblages (Casellato & Erba, 2015).

The "*Schizosphaerella* crisis" is evidenced by its drastic reduction in abundance just prior to the T-OAE black shale interval and represents the temporary breakdown of such a rock-forming taxon (Erba, 2004; Tremolada et al., 2005). Similar and coeval decreases in abundance of *S. punctulata* - and in general in nannofossil total abundances - are reported from Portugal (Mattioli et al., 2008), Spain (Fraguas et al., 2012), and France (Hermoso et al., 2012), pointing to a major shift in nannofloral assemblages at supra-regional scale.

The T-OAE perturbation also affected the biomineralisation of *Schizosphaerella*, which shows reduced sizes as documented in the Somma section (Mattioli & Pittet, 2002; Mattioli et al., 2004b, 2009). Fig. 6 illustrates the size changes measured in the Sogno Core (this study) for the interval preceding the T-OAE, within the T-OAE and in samples from the overlying interval. Both the mean and median diameter values decrease in the black shale interval, further evidencing - contemporaneously to the abundance drop - reduced calcification of *Schizosphaerella*. Such decrease in size

was also documented in Italy for the Somma section (Mattioli et al., 2004b, 2009), in France (Clemence et al., 2015), Spain (Reolid et al., 2014), and Portugal (Suan et al., 2008, 2010).

The nannoplankton patterns described above for Italian pelagic sections confirm general trends documented elsewhere, indicating stepped palaeoenvironmental perturbations culminating into the T-OAE. The extreme conditions resulting from combined warming, ocean fertilisation and possibly acidification contributed to the establishment of very stressing surface waters with dominance of opportunistic taxa. Ocean acidification might have reached threshold values at the onset of the T-OAE inducing the “*Schizosphaerella* crisis”, the drop in abundance of *M. jansae* and the temporary size reduction in *Schizosphaerella*.

Environmental stress started to affect the ocean structure, fertility and chemistry at least one million years before the T-OAE, close to the Pliensbachian/Toarcian boundary, that was a time of accelerated nannoplankton speciation, a most spectacular case for calcareous nannoplankton evolution within the Mesozoic (Bown et al., 2004; Erba, 2006). Data from Italian pelagic sections support the interpretation of the T-OAE as a nutrification episode combined with some ocean acidification exerting a direct control on phytoplankton type and abundance, and influencing species-specific biocalcification.

The late Valanginian Weissert-OAE

Eight sections covering the Weissert-OAE were analysed for C isotopic chemostratigraphy (Fig. 7). In particular, five sections were studied in the Lombardy Basin (Pusiano, Rio Corna, Capriolo, Polaveno) and on the Trento Plateau (Valle Aviana section) while the Valle del Mis and Chiaserna sections are located in the Belluno and Umbria-Marche Basins, respectively. Finally, we also

considered here the S’Ozzastru section in Sardinia, which consists of relatively shallow-water sediments deposited during flooding of a carbonate ramp. Two major papers published in the nineties still represent the sole reference of the Weissert-OAE in Italy (Lini et al., 1992; Channell et al., 1993). However, recent works at the Chiaserna (Sprovieri et al., 2006) and S’Ozzastru sections (Bottini et al., 2018) document with new data the occurrence of the Weissert carbon isotopic anomaly. It should be noticed that not all of these outcrops cover the entire OAE: the Val del Mis section records just the descending trend of the event after the C-isotope anomaly, and the S’Ozzastru section covers the initial increase of the carbon isotopic excursion (Fig. 7).

Calcareous nannofossil absolute abundances were quantified only for the Polaveno section (Erba & Tremolada, 2004), but semiquantitative data are also available for the Pusiano section (Channell et al., 1993). The Weissert-OAE interval is marked by a decline in abundance of all nannoconids, called “nannoconid decline” (sensu Channell et al., 1993), whose onset correlates with magnetochron CM12 and predates the positive $\delta^{13}\text{C}$ excursion. Nannoconid abundance resumes during the C-isotope recovery starting within magnetochron CM10N. The “nannoconid decline” interval is also characterised by higher abundance of *Diazomatolithus* throughout the entire Weissert-OAE interval. Absolute abundances of *Diazomatolithus* (Erba & Tremolada, 2004) show a symmetric increase and decrease specular to the relative decrease and increase in abundance of nannoconids. In Italian pelagic sections, the onset of the “nannoconid decline” is also marked by a peak in abundance of pentaliths (Bersezio et al., 2002; Erba & Tremolada, 2004) (Fig. 7).

The “nannoconid decline” depicted in the Tethyan sections (Channell et al., 1993; Bersezio et al., 2002;

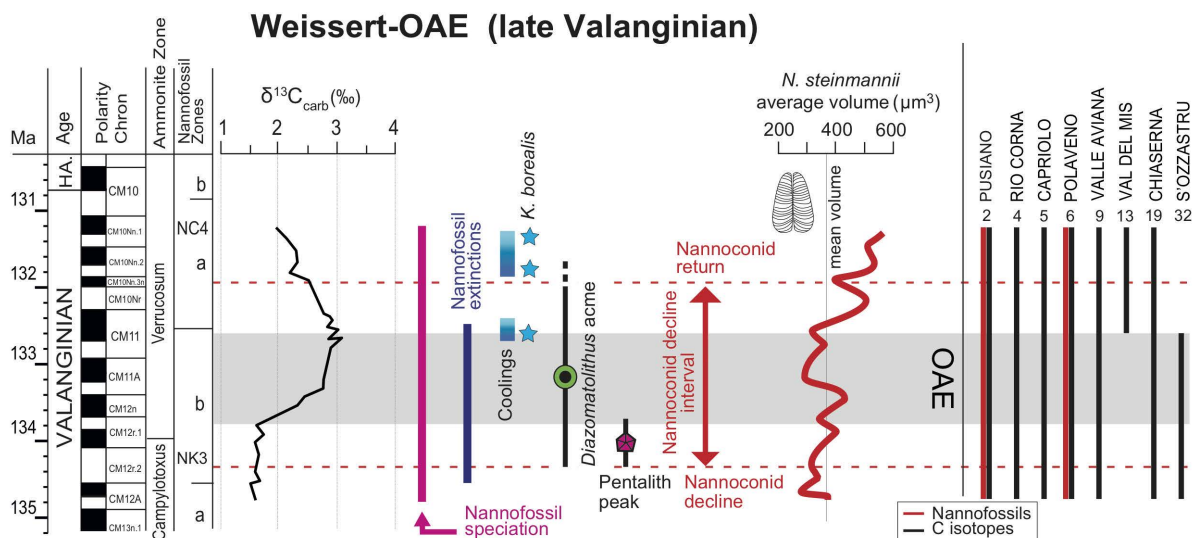


Fig. 7 - On the left: synthesis of calcareous nannofossil changes through the Weissert-OAE (ca. 134 Ma). Nannofossil origination and extinction intervals are reported as pink and blue bars, respectively. The nannoconid variations in abundance (Erba & Tremolada, 2004) and the volume of *N. steinmannii* (three point moving average of the volume, this study) are reported. The extent of the *Diazomatolithus* acme, the pentalith abundance peak and the presence of *Kokia borealis* are also represented (Bersezio et al., 2002; Erba & Tremolada, 2004). On the right: the stratigraphic extent of published (semi)quantitative nannofossil data (red bar) and available inorganic and/or organic stable carbon isotope record (black bar) is reported for each section. Section numbering as in Fig. 3. The Weissert-OAE is indicated with a grey band. The time scale is from Channell et al. (1995). Carbon isotope curve is modified after Channell et al. (1993) (Capriolo section).

Erba & Tremolada, 2004; Bottini et al., 2018) has been later documented as a global shift in the composition of nannofloral assemblages (Erba et al., 2004; Bornemann & Mutterlose, 2008; Greselle et al., 2011; Barbarin et al., 2012; Duchamp-Alphonse et al., 2014; Mattioli et al., 2014).

Morphometric analyses of *N. steinmannii* were performed for the Polaveno section (Fig. 8) to test a possible size reduction associated to the “nannoconid decline”. Collected data show that the base width and the height fluctuate independently ($R^2 = 0.31$), but that the volume is highly correlated with the base width ($R^2 = 0.81$) and to a minor extent with the height ($R^2 = 0.66$). In Fig. 7, we illustrate the volume fluctuations as the three-point moving average of the volume curve. Average volume values of ca. $300 \mu\text{m}^3$ are recorded in the interval preceding the Weissert-OAE and a moderate increase is observed at the onset of the OAE, followed by a decrease (to ca. $250 \mu\text{m}^3$) in correspondence of the climax of the $\delta^{13}\text{C}$ excursion. The interval following the Weissert-OAE is marked by a large increase in the average volume (to ca. $500 \mu\text{m}^3$) during the recovery phase. The size variations of *N. steinmannii* do not show any correspondence with fluctuations in nannoconid total abundance, indicating that these two parameters were independent and that the factor/s that caused the “nannoconid decline” did not affect the size of *N. steinmannii*, although larger specimens are observed in the recovery phase of the C-isotope curve at supraregional scale (Barbarin et al., 2012; this study).

The Italian pelagic record of the Weissert-OAE shows changes in nannofossil abundance and composition that have been also documented in France (Barbarin et al., 2012; Duchamp et al., 2014), in the Atlantic (Bornemann & Mutterlose, 2008) and in the Pacific (Erba et al., 2004) Oceans, thus demonstrating the supra-regional nature of the nannoplankton response. The Weissert-OAE differs from other Cretaceous OAEs since it was characterised by relatively cooler conditions, as for example documented by the occurrence of the nannofossil boreal species *Kokia borealis* Perch-Nielsen, 1988 at low latitudes in Romania (Melinte & Mutterlose, 2001) and in the tropical Pacific Ocean (Erba et al., 2004). Therefore, the palaeoenvironmental perturbations across the Weissert-OAE cannot be ascribed to global warming. The biocalcification crisis expressed by the “nannoconid decline” has been linked to excess CO_2 and concurrent higher fertility (Bersezio et al., 2002; Erba & Tremolada, 2004; Erba et al., 2004; Weissert & Erba, 2004). Although ocean acidification as the triggering factor of the major decrease in abundance of the heavily calcified nannoconids has been disputed (Duchamp-Alphonse et al., 2007, 2014; Barbarin et al., 2012), there is a general consensus on the

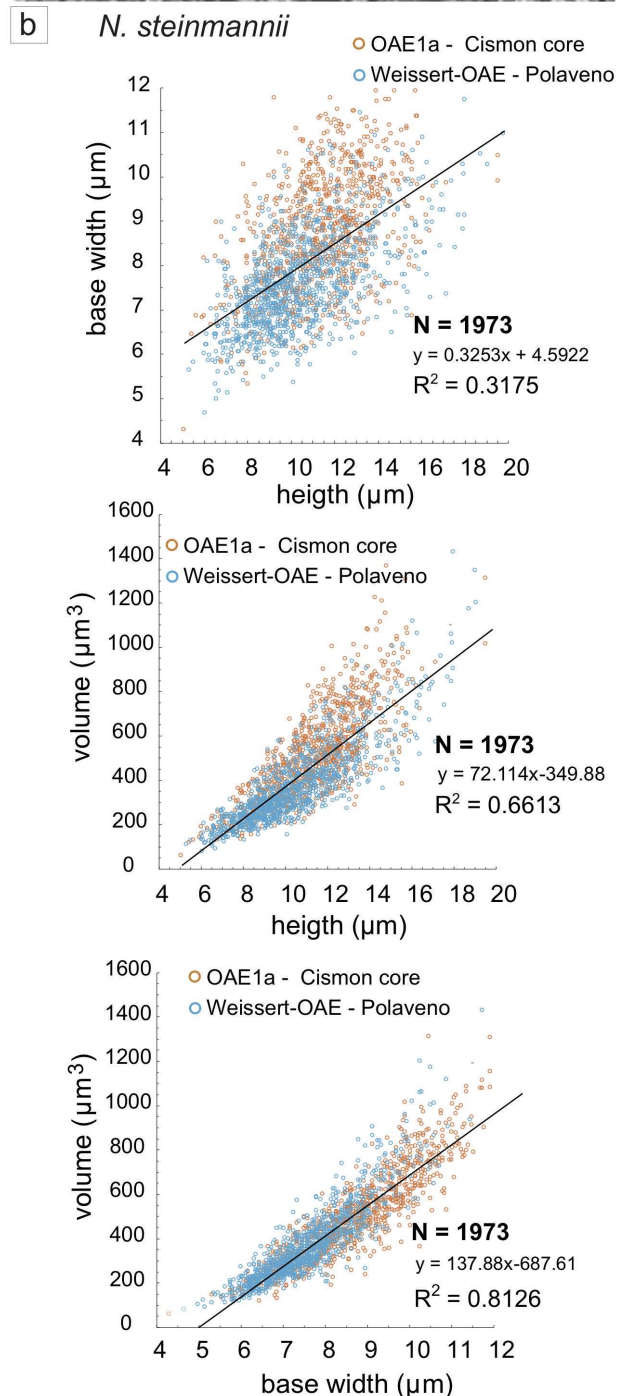
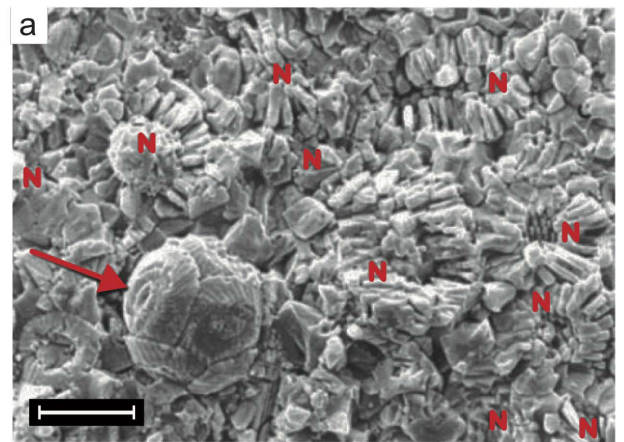


Fig. 8 - a) Scanning electron microscope image of a nannoconid-micrite from the Maiolica limestone of the Gorgo a Cerbara section. Nannoconids are marked by “N”, on the left side, indicated by the arrow, there is a coccosphere of *Watznaueria barnesiae* (Black in Black & Barnes, 1959) (after Erba, 1994); scale bar = $10 \mu\text{m}$. b) Scatter plots of *N. steinmannii* base width, height and volume with Pearson correlation coefficient (r) and the number of measurements (N). Blue circles refer to the Polaveno section (Valanginian Weissert-OAE), orange circles refer to the Cison Core (early Aptian OAE1a).

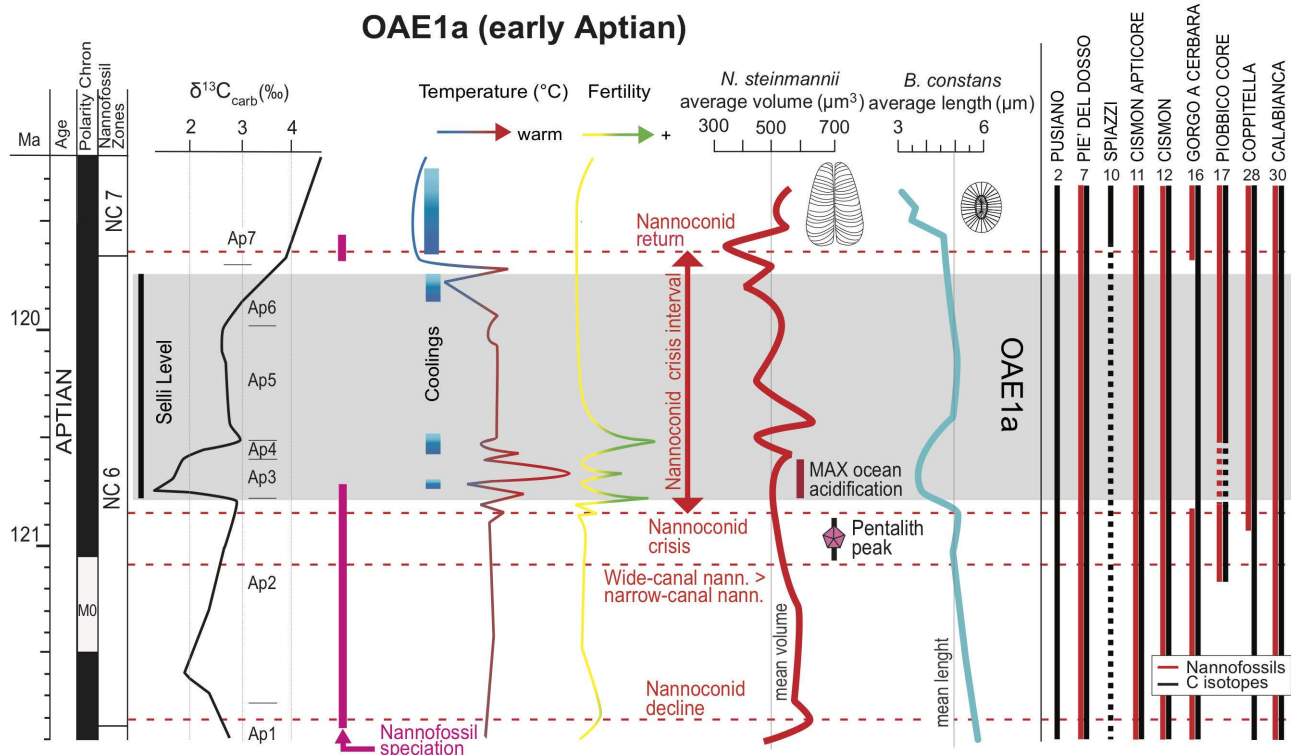


Fig. 9 - On the left: synthesis of calcareous nannofossil changes through the early Aptian OAE1a (ca. 120 Ma). Nannofossil origination intervals are reported as pink bars. The nannoconid variations in abundance (Erba & Tremolada, 2004; Bottini et al., 2015), the volume of *N. steinmannii* (three point moving average of the volume, this study) and the length of *B. constans* (three point moving average of the length; Erba et al., 2010) are reported. The pentalith abundance peak is also represented (Erba & Tremolada, 2004). Nannofossil-based temperature and nutrient indices are after Bottini et al. (2015). On the right: the stratigraphic extent of published (semi)quantitative nannofossil data (red bar) and available inorganic and/or organic stable carbon isotope record (black bar) is reported for each section. The occurrence of a hiatus is indicated with a dashed line. Section numbering as in Fig. 3. The OAE1a is indicated with a grey band. The time scale is from Malinverno et al. (2010, 2012). Carbon isotope curve is modified after Bottini et al. (2015), Cison Core (Italy). Identification of segments of the carbon isotopic anomaly across OAE1a follows Bottini et al. (2015).

role of enhanced fertility (Bersezio et al., 2002; Erba et al., 2004; Duchamp-Alphonse et al., 2007, 2014; Bornemann & Mutterlose, 2008; Barbarin et al., 2012).

The early Aptian OAE1a

Nine Italian sections record the occurrence of OAE1a as traced by carbon isotope data (Fig. 9). In particular, the Pusiano and Piè del Dosso sections in the Lombardy Basin, the Spiazzi section on the Trento Plateau, the Cison Core and outcrop in the Belluno Basin, the Gorgo a Cerbara section and the Piobbico Core in the Umbria-Marche Basin, the Coppitella section in Gargano (Puglia, southern Italy) and the Calabianca section in Sicily. The Cison APTICORE is the most studied record for OAE1a in Italy (Tab. 3). In fact, following the first work of Erba et al. (1999), a large amount of published literature has continuously extended and/or refined the C_{carb} and C_{org} chemostratigraphy, highlighting the importance of this core as a fundamental reference for the OAE1a interval. The distribution of the various sections allows for comparisons of the occurrence and extent of OAE1a in different basins. However, it must be noticed that not all the published records are complete, in particular the Spiazzi section documents only a small portion of the event, as it preserves just the uppermost part of the carbon isotopic anomaly, while a hiatus corresponds to the Ap3

and Ap4 intervals of the carbon excursion in the Piobbico Core (Bottini et al., 2015).

Quantitative abundance data of nannofossil assemblages of the upper Barremian-lower Aptian are available for the Piè del Dosso, Cison outcrop and Core, Gorgo a Cerbara, Piobbico Core, Coppitella and Calabianca (Erba, 1994; Luciani et al., 2001; Bellanca et al., 2002; Erba & Tremolada, 2004; Bottini et al., 2015). Slightly before the onset of OAE1a, the “nannoconid crisis” documents a major decrease of nannofossil calcite production. It represents the culmination of a trend initiated close to the Barremian/Aptian boundary with the “nannoconid decline” associated with the appearance of small taxa. Together these changes seem to testify the response of calcareous nannoplankton to increased CO_2 and metal enrichment (Erba et al., 2015). The “nannoconid crisis” corresponds to a more severe biocalcification failure, with a drop in pelagic biogenic calcite production of ~80% under excess CO_2 , enhanced nutrient availability, global warming and possibly ocean acidification (Erba et al., 2010). Despite the major temporary crisis during OAE1a, the nannoconids were able to survive, presumably in sufficiently shielded ecological niches, and to partially recover to pre-crisis abundance and palaeofluxes when palaeoenvironmental conditions ameliorated (Erba et al., 2015).

ITALIAN PELAGIC SECTIONS WITH NANNOFOSSIL AND CARBON ISOTOPIC DATA FOR OAE1a				
n.	Locality	Reference	Nannofossils	$\delta^{13}\text{C}$
2.	Pusiano (Lombardy Basin, northeastern Italy)	Keller et al., 2011		•
7.	Piè del Dosso (Lombardy Basin, northeastern Italy)	Erba, 1994	•	
		Giorgioni et al., 2015		•
10.	Spiazzi (Trento Plateau, northeastern Italy)	Weissert et al., 1985		•
11.	Cismon APTICORE (Belluno Basin, northeastern Italy)	Premoli Silva et al., 1999	•	
		Erba et al., 1999		•
		Tremolada & Erba, 2002	•	
		van Breugel et al., 2007		•
		Erba & Tremolada, 2004	•	
		Mehay et al., 2009	•	•
		Erba et al., 2010	•	•
		Giorgioni et al., 2015		•
		Bottini et al., 2015	•	
		This work	•	
12.	Cismon (Belluno Basin, northeastern Italy)	Weissert et al., 1985		•
		Erba, 1994	•	
		Menegatti et al., 1998		•
16.	Gorgo a Cerbara (Umbria-Marche, central Italy)	Coccioni et al., 1992	•	
		Erba, 1994	•	
		Erbacher et al., 1996		•
		Tejada et al., 2009		•
		Stein et al., 2011		•
17.	Piobbico Core (Umbria-Marche, central Italy)	Premoli Silva et al., 1989	•	
		Erba, 1994	•	
		Erba et al., 2015		•
		Bottini et al., 2015	•	
28.	Coppitella (Gargano, southern Italy)	Luciani et al., 2001	•	•
30.	Calabianca (Sicily, southern Italy)	Bellanca et al., 2002	•	•

Tab. 3 - Compilation of papers documenting quantitative nannofossil and carbon isotope data for the OAE1a interval.

Morphometric data of *B. constans*, obtained for the uppermost Barremian through Cenomanian interval of Italian sections (Erba et al., 2010; Faucher et al., 2017; this work), show that coccolith length and width are directly correlated ($R^2 = 0.80$) (Fig. 10), thus we only comment the fluctuations of the mean length, reported as the three-point moving average of the mean length curve. In the Cismon Core the coccolith length/width Pearson correlation is very high ($R^2 = 0.90$); *B. constans* shows a marked reduction in size in correspondence of the onset of the OAE1a and minimum average size (ca. 3 μm) was reached in the core of the negative $\delta^{13}\text{C}$ segment Ap3 (Fig. 9). The mean *B.*

constans length increases across segments Ap4 to Ap6 and remains relatively stable up to the end of OAE1a. A minor decrease in the average coccolith size is detected in segment Ap7.

Morphometric analyses of *N. steinmannii* performed in the Cismon Core (this study) highlight rather stable sizes through OAE1a. As for the Weissert-OAE, the base width and height are not correlated but there is a correlation between the base width and the height with the volume (Fig. 8). The average volume is above 500 μm^3 prior to OAE1a and shows a minor decrease during the event. The only interval characterised by relatively smaller specimens

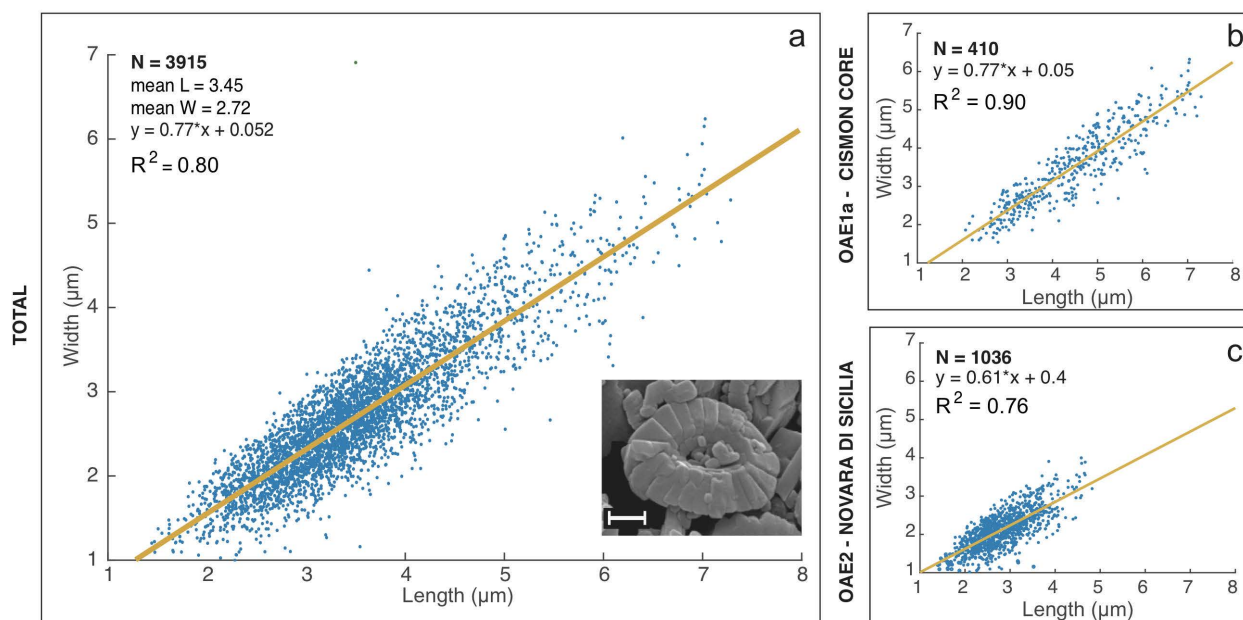


Fig. 10 - Scatter plots of *B. constans* length and width with Pearson correlation coefficient (r) and the number of measurements (N). a) Scatter plots of *B. constans* length and width measured in uppermost Barremian-Cenomanian Italian sections (Erba et al., 2010; Faucher et al., 2017; this work); scale bar = 1 μ m. b) Scatter plots of *B. constans* length and width measured across the early Aptian OAE1a in the Cismone Core (Erba et al., 2010). c) Scatter plots of *B. constans* across the Cenomanian/Turonian OAE2 from Novara di Sicilia section (Faucher et al., 2017).

(average volume comprised between 300 and 400 mm^3) coincides with the end of OAE1a (segments Ap6-base Ap7) (Fig. 9) which is followed by an interval of increased sizes during $\delta^{13}\text{C}$ segment Ap7 (Fig. 9). The average volume of *N. steinmannii* in the early Aptian (500 mm^3) is relatively higher compared to the Weissert-OAE (380 mm^3). But, similarly to the Valanginian Weissert-OAE, the *N. steinmannii* mean size does not show correlation with the nannoconid total abundance. In the specific case of OAE1a, the volume fluctuations of *N. steinmannii* do not follow the size variations displayed by *B. constans* coccoliths.

The latest Barremian “nannoconid decline” and early Aptian “nannoconid crisis” have been documented at global scale (Erba, 1994, 2004; Erba et al., 2015) and are interpreted as the result of concurrent higher fertility and excess CO_2 that would have negatively affected the biocalcification process in calcareous nannoplankton (Erba & Tremolada, 2004; Erba et al., 2010, 2015). The coincidence of the “nannoconid decline” and “nannoconid crisis” with trace metal enrichments was further explained by hydrothermal activity releasing large quantities of biolimiting and/or toxic trace elements (Erba et al., 2015). The maximum perturbation was reached in the core of the negative $\delta^{13}\text{C}$ anomaly, when the highest temperatures, highest surface water fertility, the maximum ocean acidification and the maximum reduction of coccolith size occurred. The nannoconids responded to these perturbations with a severe reduction in the total abundance, but not with significant size variations.

The latest Cenomanian OAE2

Ten sections reporting the carbon isotope excursion for the OAE2 in Italy are described in the literature (Fig. 11). Most sections are located in the Umbria-

Marche Basin (Furlo, Gorgo a Cerbara, Monte Petrano, Bottaccione, Contessa sections, and Gubbio S2 Core), but other outcrops document the OAE2 positive C-isotope excursion in the Belluno Basin (Cismone section) and in Sicily (Novara di Sicilia, Calabianca and Guidaloca sections). Among all, the Bottaccione area represents a cornerstone for OAE2 C-isotope chemostratigraphy in Italy (Tab. 4). In fact, following the seminal work of Scholle & Arthur (1980), many papers in the past 40 years have continuously documented the occurrence of the $\delta^{13}\text{C}$ positive anomaly characterising OAE2 in the Gubbio succession. Even if the Umbria-Marche Basin remains a key-area for the stratigraphy of OAE2, recent advances in the $\delta^{13}\text{C}$ chemostratigraphy (Gambacorta et al., 2015, 2016), suggest that in the Furlo, Contessa-Gubbio S2 Core, Monte Petrano and Gorgo a Cerbara sections a regional hiatus elides most of the C-isotope anomaly, namely the “plateau”, the “c” peak and the first part of the recovery. Therefore, the OAE2 stratigraphic record in these sections was proved incomplete (Fig. 11). In Sicily, just the Calabianca section contains the entire $\delta^{13}\text{C}$ excursion, as the Novara di Sicilia and Guidaloca sections cover only the lower and uppermost part of the event, respectively.

Quantitative analyses of calcareous nannofloras are scanty for Italian sections, because the Bonarelli Level is typically barren of calcareous nannofossils. Changes in abundance across OAE2 were obtained for the Bottaccione section (Erba, 2004) and morphometric data were documented by Faucher et al. (2017) for the Novara di Sicilia section. In addition, quantitative nannofossil data are available for the intervals below and above the Bonarelli Level of the Furlo and Monte Petrano sections. The absence or extremely rareness of calcareous nannofossils across the OAE2 black shales of the Bonarelli Level is attributed to extreme acidification

ITALIAN PELAGIC SECTIONS WITH NANNOFOSSIL AND CARBON ISOTOPIC DATA FOR OAE2			
n.	Locality	Reference	$\delta^{13}\text{C}$
12.	Cismon (Belluno Basin, northeastern Italy)	Gambacorta et al., 2015	•
15.	Furlo (Umbria-Marche, central Italy)	Mort et al., 2007 Jenkyns et al., 2007 Gambacorta et al., 2015 Bottini & Erba, 2018	• • • •
16.	Gorgo a Cerbara (Umbria-Marche, central Italy)	Kuroda et al., 2007	•
18.	Monte Petrano (Umbria-Marche, central Italy)	Erbacher et al., 1996 Gambacorta et al., 2015 Bottini & Erba, 2018	• • •
22.	Bottaccione Gorge (Umbria-Marche, central Italy)	Scholle & Arthur, 1980 Renard, 1986 Arthur et al., 1988 Corfield et al., 1991 Erba, 1994 Jenkyns et al., 1994 Scopelliti et al., 2008 Sprovieri et al., 2013	• • • • • • • •
23.	Gubbio - S2 Core (Umbria-Marche, central Italy)	Tsikos et al., 2004	•
24.	Contessa (Umbria-Marche, central Italy)	Stoll & Schrag, 2000	•
29.	Novara di Sicilia (northwestern Sicily, southern Italy)	Scopelliti et al., 2008 Faucher et al., 2017	• •
30.	Calabianca (northwestern Sicily, southern Italy)	Scopelliti et al., 2004 Scopelliti et al., 2008	• •
31.	Guidaloca (northwestern Sicily, southern Italy)	Scopelliti et al., 2004	•

Tab. 4 - Compilation of papers documenting quantitative nannofossil and carbon isotope data for the OAE2 interval.

conditions (Erba, 2004). A drop in nannofossil abundance and species richness has been documented worldwide (Nederbragt & Fiorentino, 1999; Hardas & Mutterlose, 2007; Linnert et al., 2010, 2011; Corbett & Watkins, 2013) and interpreted as the result of eutrophic conditions, perhaps combined with trace metal enrichments in surface water. These factors of palaeoenvironmental stress could have favored phytoplanktonic group other than calcareous nannoplankton (Erba, 2004; Lignum et al., 2007; Linnert et al., 2010; Faucher et al., 2017). Indeed, *Biscutum* is interpreted as a higher fertility taxon, but its drop in abundance might be evidence of trophic conditions above threshold values for calcareous nannoplankton during OAE2 (Erba, 2004).

Morphometric data of *B. constans* across the latest Cenomanian OAE2 in the Novara di Sicilia section, integrated with those gathered for the Eastbourne section (Faucher et al., 2017), are represented in Fig. 11. Coccoliths of *B. constans* show significant variations in

size as traced by length and width. These two parameters are directly correlated ($R^2 = 0.76$) (Fig. 10), thus we only comment the fluctuations of the mean length, as represented in the smoothed curve of Fig. 11. At the OAE2 onset, *B. constans* shows a first decrease in size, followed by an increase of coccolith size in $\delta^{13}\text{C}$ peak "a". A further size decrease culminates with dwarfism around $\delta^{13}\text{C}$ peak "b", where the smallest coccoliths are recorded (ca. 1.5 mm). Similar and coeval trends have been documented in a variety of settings as a biocalcification response to palaeoenvironmental global stress. However, at Novara di Sicilia, *B. constans* coccoliths have the most reduced sizes compared to other sections: this seems to depict a trend of declining average coccolith size with decreasing latitude (Faucher et al., 2017).

Fluctuations of calcareous nannofossil abundance and size of selected taxa across the latest Cenomanian OAE2 are interpreted as caused by global warming, interrupted by the cooling interlude of the Plenus Cold

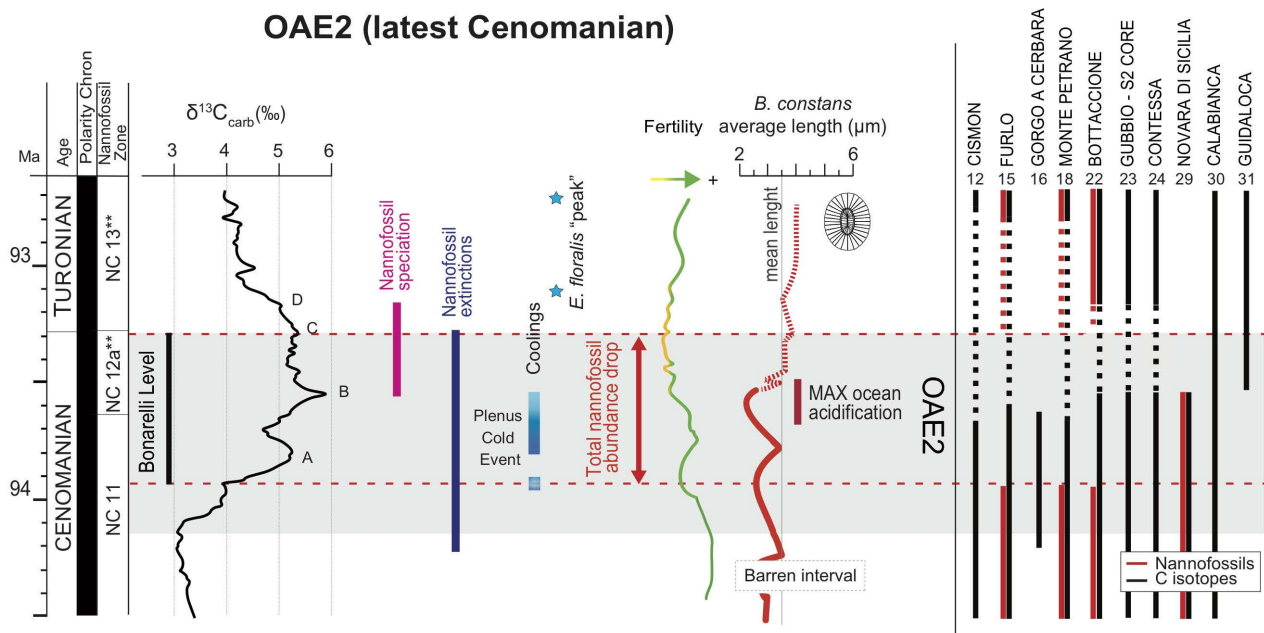


Fig. 11 - On the left: synthesis of calcareous nannofossil changes through the latest Cenomanian OAE2 (ca. 94 Ma). Nannofossil origination and extinction intervals are reported as pink and blue bars, respectively. The total nannofossil abundance variations (from Gubbio section, Erba, 2004) and the length of *B. constans* (three point moving average of the mean length, Faucher et al., 2017) are reported. Nannofossil based-nutrient index and peaks of *Eprolithus floralis* (Stradner, 1962) are from Erba (2004). Cooling intervals are from Jenkyns et al. (2017). On the right: the stratigraphic extent of published (semi)quantitative nannofossil data (red bar) and available inorganic and/or organic stable carbon isotope record (black bar) is reported for each section. The occurrence of a hiatus is indicated with a dashed line. Considering the proximity of the sites, we assume an extent of the hiatus for the Contessa and Bottaccione Gorge sections equal to that observed in the Gubbio S2 Core. Section numbering as in Fig. 3. The OAE2 is indicated with a grey band. The time scale is modified after Gradstein et al. (2012). Carbon isotope curve is modified after Tsikos et al. (2004), Eastbourne section (UK). Identification of individual peaks of the carbon isotopic anomaly across OAE2 follows Voigt et al. (2007).

Event (Gale & Christensen, 1996; Gale et al., 2019), changes in ocean fertility and chemistry. The short return to larger *B. constans* coccoliths around $\delta^{13}\text{C}$ peak "a" occurs in the Plenus Cold Event: a cool-water preference was implied for *B. constans* (Lees et al., 2005) and may explain its increase in size during the cooling interval. The subsequent *B. constans* dwarfism correlates with the maximum ocean perturbation with metal enrichments, temperature rise and probably ocean acidification due to excess CO_2 (Erba, 2004; Snow et al., 2005; Jarvis et al., 2011; Du Vivier et al., 2015; Faucher et al., 2017). Only a partial return to pre-OAE2 sizes was observed in *B. constans* coccoliths during the C-isotope recovery phase following $\delta^{13}\text{C}$ peak "d", suggesting the persistence of stressing conditions in the earliest Turonian.

CONCLUDING REMARKS

Our synthesis points out that Italian pelagic sections are key to quantify changes in calcareous nannoplankton during times of highly perturbed conditions associated with OAEs, as evidenced by $\delta^{13}\text{C}$ anomalies testifying discrete global alterations of the C cycle. Indeed, in addition to extreme climatic conditions and oceanic fertilisation, OAEs were also times of altered chemistry making calcification difficult. It is possible that volcanically driven excess CO_2 in the ocean/atmosphere system (Jenkyns, 2010) induced ocean acidification (Erba et al., 2010) and caused crises of the dominant rock-forming

calcareous nannoplankton forms. This seems the case for the "*Schizosphaerella* crisis", the "nannoconid decline" and the "nannoconid crisis" during the early Toarcian T-OAE, the late Valanginian Weissert-OAE and the early Aptian OAE1a, respectively. An even more dramatic drop in nannofossil abundance characterises the latest Cenomanian OAE2, marked by a widespread biocalcification failure of calcareous nannoplankton taxa.

In addition to major changes in nannofossil abundance, a species-specific decrease in size has been detected for most OAEs, specifically for *Schizosphaerella* across the T-OAE and *B. constans* in the interval of maximum perturbation of both OAE1a and OAE2. Size of *N. steimannii*, instead, does not show significant variations across the Weissert-OAE and OAE1a. We underline that none of the taxa experiencing a calcification crisis and/or showing a size decrease got extinct: they recovered when the palaeoenvironment returned to a pre-perturbation state, although the calcareous nannoplankton return to normal conditions occurred much slower than their response to environmental stress at the beginning of the OAE disturbance. After the T-OAE and OAE1a, schizosphaerellids and nannoconids resumed in abundance, although nannofossil assemblages changed to a different composition. This was also due to originations of new species starting some one million years before the onset of the T-OAE and OAE1a and continuing through the events (Figs 5 and 9), indicating that some calcareous nannoplankton taxa could overcome the stressing phase, perhaps by resorting to innovative pathways of

calcification. These speciation episodes developed quickly, at an average rate of one first occurrence every 100–200 k years, with no accompanying increase in extinction rate, suggesting resilience of this phytoplankton group.

The Italian pelagic record shows that the response of calcareous nannoplankton to palaeoenvironmental perturbations of the Weissert-OAE and OAE2 was significantly different. The Valanginian “nannoconid decline” was gradual and less pronounced, as it was the recovery phase, while in the late Cenomanian the dramatic reduction in nannofossil total abundance is as sudden as the recovery after OAE2. As far as nannoplankton evolutionary patterns and rates are concerned, the response to the Weissert-OAE and OAE2 was different between the two events and also with respect to the T-OAE and OAE1a. During the late Valanginian-early Hauterivian (Fig. 7), a few first occurrences followed each other slowly, about one every million years. Across OAE2, instead, extinctions occurred with a rate of one every 100–200 k years at the onset or at the end of the event, while some originations are recorded from the middle part of OAE2 and continued afterwards (Fig. 11).

In conclusion, OAEs perturbations are fully recorded in pelagic micrites by shifts in abundance of calcareous nannofossils and specifically of rock-forming taxa. The same taxa partly and gradually resumed when palaeoecosystem conditions ameliorated. Changes in biocalcification are further documented by species-specific reduction in size under maximum stress during OAEs. The role of palaeoenvironmental pressure on calcareous nannoplankton evolution during the early Toarcian T-OAE, late Valanginian Weissert-OAE, early Aptian OAE1a and latest Cenomanian OAE2, if any, was not univocal, but in general resulted in the origination of new taxa.

ACKNOWLEDGEMENTS

We thank our Colleagues that contributed with thoughtful discussions to the comprehension of Jurassic and Cretaceous OAEs, particularly J.E.T. Channell, H. Jenkyns, I. Premoli Silva, and H. Weissert: with them we shared field work, especially in Italy, and scientific debates. M. Parente and I. Premoli Silva provided insightful reviews complementing the Editors’ criticism. This synthesis benefitted, at various stages, of the financial support by MIUR-PRIN2011(2010X3PP8J) awarded to E.E. and SIR-2014 (MIUR-Scientific Independence of young Researchers) to C.B.

REFERENCES

- Abramovich S., Keller G., Stüben D. & Berner Z. (2003). Characterization of late Campanian and Maastrichtian planktonic foraminiferal depth habitats and vital activities based on stable isotopes. *Palaeogeography, Palaeoclimatology, Palaeoecology*, 202: 1–29.
- Arthur M.A., Dean W.E. & Pratt L.M. (1988). Geochemical and climatic effects of increased marine organic carbon burial at the Cenomanian/Turonian boundary. *Nature*, 335: 714–717.
- Arthur M.A., Jenkyns H.C., Brumsack H.-J. & Schlanger S.O. (1990). Stratigraphy, geochemistry, and paleoceanography of organic-carbon-rich Cretaceous sequences. In Ginsburg R.N. & Beaudoin B. (eds), *Cretaceous Resources, Events and Rhythms*, NATO ASI Series, 304: 75–119.
- Arthur M.A. & Schlanger S.O. (1979). Cretaceous “oceanic anoxic events” as causal factors in development of reef-reservoired giant oil fields. *AAPG Bulletin*, 63: 870–885.
- Barbarin N., Bonin A., Mattioli E., Pucéat E., Cappetta H., Gréselle B., Pittet B., Vennin E. & Joachimski M. (2012). Evidence for a complex Valanginian nannoconid decline in the Vocontian basin (South East France). *Marine Micropaleontology*, 84: 37–53.
- Bellanca A., Erba E., Neri R., Premoli Silva I., Sprovieri M., Tremolada F. & Verga D. (2002). Paleocyanographic significance of the Tethyan “Livello Selli” (Early Aptian) from the Hybla Formation, northwestern Sicily: biostratigraphy and high-resolution chemostratigraphic records. *Palaeogeography, Palaeoclimatology, Palaeoecology*, 185: 175–196.
- Bersezio R., Erba E., Gorza M. & Riva A. (2002). Berriasian-Aptian black shales of the Maiolica Formation (Lombardian Basin, Southern Alps, northern Italy): Local to global events: *Palaeogeography, Palaeoclimatology, Palaeoecology*, 180: 253–275.
- Black M. & Barnes B. (1959). The structure of Coccoliths from the English Chalk. *Geological Magazine*, 96: 321–328.
- Bornemann A. & Mutterlose J. (2008). Calcareous nannofossil and $\delta^{13}\text{C}$ records from the Early Cretaceous of the Western Atlantic Ocean: evidence for enhanced fertilization across the Berriasian-Valanginian transition. *Palaios*, 23: 821–832.
- Bottini C., Dieni I., Erba E. & Massari F. (2018). The Valanginian Weissert Oceanic Anoxic Event Recorded in Central-Eastern Sardinia (Italy). *Rivista Italiana di Paleontologia e Stratigrafia*, 124: 617–637.
- Bottini C. & Erba E. (2018). Mid-Cretaceous paleoenvironmental changes in the western Tethys. *Climate of the Past*, 14: 1147–1163.
- Bottini C., Erba E., Tiraboschi D., Jenkyns H.C., Schouten S. & Sinninghe Damsté J.S. (2015). Climate variability and ocean fertility during the Aptian Stage. *Climate of the Past*, 11: 383–402.
- Bown P.R., Lees J.A. & Young J.R. (2004). Calcareous nannoplankton evolution and diversity through time. In Winter A. & Siesser W.G. (eds), *Coccolithophores*: 481–508.
- Breheret I.G. (1983). Sur des niveaux de black shales dans l’Albien inférieur et moyen du domaine vocontien (sud-est de la France): étude de nanofacies et signification des palaeoenvironnements. *Bulletin du Muséum National d’Histoire Naturelle, Paris*, 5: 113–159.
- Bucefalo Palliani R., Cirilli S. & Mattioli E. (1998). Phytoplankton response and geochemical evidence of the lower Toarcian relative sea level rise in the Umbria-Marche basin (Central Italy). *Palaeogeography, Palaeoclimatology, Palaeoecology*, 142: 33–50.
- Casellato C.E. & Erba E. (2015). Calcareous nannofossil biostratigraphy and paleoceanography of the Toarcian Oceanic Anoxic Event at Colle di Sogno section (Southern Alps, Italy). *Rivista Italiana di Paleontologia e Stratigrafia*, 105: 343–376.
- Channell J.E.T., Erba E. & Lini A. (1993). Magnetostratigraphic calibration of the Late Valanginian carbon isotope event in pelagic limestones from Northern Italy and Switzerland. *Earth Planetary Science Letters*, 118: 145–166.
- Channell J.E.T., Erba E., Nakanishi M. & Tamaki K. (1995). Late Jurassic–Early Cretaceous time scales and oceanic magnetic anomaly block models. In Berggren W.A. et al. (eds), *Geochronology, time scales and global stratigraphic correlation. SEPM (Society for Sedimentary Geology) Special Publication*, 54: 51–63.
- Claps M., Erba E., Masetti D. & Melchiorri F. (1995). Milankovitch-type cycles recorded in Toarcian black shales from the Belluno Trough (Southern Alps, Italy). *Memorie di Scienze Geologiche*, 47: 179–188.
- Clémence M.E., Gardin S. & Bartolini A. (2015). New insights in the pattern and timing of the Early Jurassic calcareous nannofossil crisis. *Palaeogeography, Palaeoclimatology, Palaeoecology*, 427: 100–108.

- Cobianchi M. & Picotti V. (2001). Sedimentary and biological response to sea-level and palaeoceanographic changes of a Lower-Middle Jurassic Tethyan platform margin (Southern Alps, Italy). *Palaeogeography, Palaeoclimatology, Palaeoecology*, 169: 219-244.
- Coccioni R., Erba E. & Premoli Silva I. (1992). Barremian–Aptian calcareous plankton biostratigraphy from the Gorgo a Cerbara section (Marche, Central Italy) and implications for plankton evolution. *Cretaceous Research*, 13: 517-537.
- Coccioni R., Nesci O., Tramontana M., Wezel F.C. & Moretti E. (1987). Descrizione di un livello-guida “radiolaritico-bituminoso-ittiolitico” alla base delle Marne a Fucoidi nell’Appennino Umbro-Marchigiano. *Bollettino della Società Geologica Italiana*, 106: 183-192.
- Corbett M.J. & Watkins D.K. (2013). Calcareous nannofossil paleoecology of the mid-Cretaceous Western Interior Seaway and evidence of oligotrophic surface waters during OAE2. *Palaeogeography, Palaeoclimatology, Palaeoecology*, 392: 510-523.
- Corfield R.M., Cartlidge J.E., Premoli-Silva I. & Housley R.A. (1991). Oxygen and carbon isotope stratigraphy of the Palaeogene and Cretaceous limestones in the Bottaccione Gorge and the Contessa Highway sections, Umbria, Italy. *Terra Nova*, 3: 414-422.
- Dal Piaz G. (1907). Le Alpi Feltrine. *Memorie del Reale Istituto Veneto di Scienze Lettere ed Arti*, 27: 1-176.
- Deflandre G. & Dangeard L. (1938). *Schizosphaerella*, un nouveau microfossile méconnu du Jurassique moyen et supérieur. *Comptes Rendus (Hebdomadaires des Séances) de l’Académie des Sciences Paris*, 207: 1115-1117.
- Dromart G., Garcia J.-P., Gaumet F., Picard S., Rousseau M., Atrops F., Lecuyer C. & Sheppard S.M.F. (2003). Perturbation of the carbon cycle at the Middle/Late Jurassic transition: geological and geochemical evidence. *American Journal of Science*, 303: 667-707.
- Du Vivier A.D., Jacobson A.D., Lehn G.O., Selby D., Hurtgen M.T. & Sageman B.B. (2015). Ca isotope stratigraphy across the Cenomanian–Turonian OAE 2: links between volcanism, seawater geochemistry, and the carbonate fractionation factor. *Earth and Planetary Science Letters*, 416: 121-131.
- Duchamp-Alphonse S., Gardin S. & Bartolini A. (2014). Calcareous nannofossil response to the Weissert episode (Early Cretaceous): Implications for palaeoecological and palaeoceanographic reconstructions. *Marine Micropaleontology*, 113: 65-78.
- Duchamp-Alphonse S., Gardin S., Fiet N., Bartolini A., Blamart D. & Pagel M. (2007). Fertilization of the northwestern Tethys (Vocontian basin, SE France) during the Valanginian carbon isotope perturbation: evidence from calcareous nannofossils and trace element data. *Palaeogeography, Palaeoclimatology, Palaeoecology*, 243: 132-151.
- Erba E. (1994). Nannofossils and superplumes: the early Aptian nannoconid crisis. *Paleoceanography*, 9: 483-501.
- Erba E. (2004). Calcareous nannofossils and Mesozoic oceanic anoxic events. *Marine Micropaleontology*, 52: 85-106.
- Erba E. (2006). The first 150 million years history of calcareous nannoplankton: biosphere–geosphere interactions. *Palaeogeography, Palaeoclimatology, Palaeoecology*, 232: 237-250.
- Erba E., Bartolini A. & Larson R.L. (2004). Valanginian Weissert oceanic anoxic event. *Geology*, 32: 149-152.
- Erba E., Bottini C., Weissert H.J. & Keller C.E. (2010). Calcareous nannoplankton response to surface-water acidification around Oceanic Anoxic Event 1a. *Science*, 329: 428-432.
- Erba E., Channell J.E.T., Claps M., Jones C., Larson R.L., Opdyke B., Premoli Silva I., Riva A., Salvini G. & Torricelli S. (1999). Integrated stratigraphy of the Cismon Apticore (Southern Alps, Italy): A “reference section” for the Barremian–Aptian interval at low latitudes. *Journal of Foraminiferal Research*, 29: 371-391.
- Erba E., Duncan R.A., Bottini C., Tiraboschi D., Weissert H., Jenkyns H.C. & Malinverno A. (2015). Environmental consequences of Ontong Java Plateau and Kerguelen Plateau volcanism. *Geological Society of America Special Papers*, 511: 271-303.
- Erba E. & Tremolada F. (2004). Nannofossil carbonate fluxes during the Early Cretaceous: phytoplankton response to nutrification episodes, atmospheric CO₂ and anoxia. *Paleoceanography*, 19: 1-18.
- Erbacher J., Thurow J. & Littke R. (1996). Evolution patterns of radiolaria and organic matter variations: A new approach to identify sea-level changes in mid-Cretaceous pelagic environments. *Geology*, 24: 499-502.
- Farinacci A. (1964). Microrganismi dei calcari ‘Maiolica’ e ‘Scaglia’ osservati al microscopio elettronico (nannoconi e coccolithophoridi). *Bollettino della Società Paleontologica Italiana*, 3: 172-181.
- Faucher G., Erba E., Bottini C. & Gambacorta G. (2017). Calcareous nannoplankton response to the latest Cenomanian Oceanic Anoxic Event 2 perturbation. *Rivista Italiana di Paleontologia e Stratigrafia*, 123: 159-176.
- Fraguas Á., Comas-Rengifo M.J., Gómez J.J. & Goy A. (2012). The calcareous nannofossil crisis in Northern Spain (Asturias province) linked to the Early Toarcian warming-driven mass extinction. *Marine Micropaleontology*, 94: 58-71.
- Gaetani M. & Poliani G. (1978). Il Toarciano ed il Giurassico medio in Albenza. *Rivista Italiana di Paleontologia e Stratigrafia*, 91: 295-320.
- Gale A.S. & Christensen W.K. (1996). Occurrence of the belemnite *Actinocamax plenus* in the Cenomanian of SE France and its significance. *Bulletin of the Geological Society of Denmark*, 43: 68-77.
- Gale A.S., Jenkyns H.C., Tsikos H., van Breugel Y., Sinnighe Damste J.S., Bottini C., Erba E., Russo F., Falzoni F., Petrizzo M.R., Dickson A.J. & Wray D.S. (2019). High-resolution bio- and chemostratigraphy of an expanded record of Oceanic Anoxic Event 2 (Late Cenomanian–Early Turonian) at Clot Chevalier, near Barrême, SE France (Vocontian Basin, SE France). *Newsletters on Stratigraphy*, 52: 97-129.
- Gambacorta G., Bersezio R., Weissert H. & Erba E. (2016). Onset and demise of Cretaceous oceanic anoxic events: The coupling of surface and bottom oceanic processes in two pelagic basins of the western Tethys. *Paleoceanography*, 31: 732-757.
- Gambacorta G., Jenkyns H.C., Russo F., Tsikos H., Wilson P.A., Faucher G. & Erba E. (2015). Carbon- and oxygen-isotope records of mid-Cretaceous Tethyan pelagic sequences from the Umbria-Marche and Belluno Basins (Italy). *Newsletters on Stratigraphy*, 48: 299-323.
- Giorgioni M., Keller C.E., Weissert H., Hochuli P.A. & Bernasconi S.M. (2015). Black shales—from coolhouse to greenhouse (early Aptian). *Cretaceous Research*, 56: 716-731.
- Górka H. (1957). Les Coccolithophoridés du Maestrichtien supérieur de Pologne. *Acta Palaeontologica Polonica*, 2: 239-284.
- Gradstein F.M., Ogg J.G., Schmitz M.D. & Ogg G.M. (2012). The Geologic Time Scale 2012. 1176 pp. Elsevier B.V., Amsterdam.
- Gréselle B., Pittet B., Mattioli E., Joachimski M., Barbarin N., Riquier L., Reboulet S. & Pucéat E. (2011). The Valanginian isotope event: a complex suite of palaeoenvironmental perturbations. *Palaeogeography, Palaeoclimatology, Palaeoecology*, 306: 41-57.
- Hardas P. & Mutterlose J. (2007). Calcareous nannofossil assemblages of Oceanic Anoxic Event 2 in the equatorial Atlantic: Evidence of an eutrophication event. *Marine Micropaleontology*, 66: 52-69.
- Hermoso M., Minoletti F., Rickaby R.E., Hesselbo S.P., Baudin F. & Jenkyns H.C. (2012). Dynamics of a stepped carbon isotope excursion: Ultra high-resolution study of Early Toarcian environmental change. *Earth and Planetary Science Letters*, 319: 45-54.
- Hesselbo S.P., Gröcke D., Jenkyns H.C., Bjerrum C.J., Farrimond P., Bell H.S.M. & Green O.R. (2000). Massive dissociation of gas hydrate during a Jurassic oceanic anoxic event. *Nature*, 406: 392-395.

- Hesselbo S.P., Jenkyns H.C., Duarte L.V. & Oliveira L.C.V. (2007). Carbon-isotope record of the Early Jurassic (Toarcian) Oceanic Anoxic Event from fossil wood and marine carbonate (Lusitanian Basin, Portugal). *Earth and Planetary Science Letters*, 253: 455-470.
- Jarvis I., Gale A.S., Jenkyns H.C. & Pearce M.A. (2006). Secular variation in Late Cretaceous carbon isotopes: a new $\delta^{13}\text{C}$ carbonate reference curve for the Cenomanian–Campanian (99.6–70.6 Ma). *Geological Magazine*, 143: 561-608.
- Jarvis I., Lignum J.S., Gröcke D.R., Jenkyns H.C. & Pearce M.A. (2011). Black shale deposition, atmospheric CO_2 drawdown, and cooling during the Cenomanian–Turonian Oceanic Anoxic Event. *Paleoceanography*, 26: PA3201.
- Jarvis I., Mabrouk A., Moody R.T.J. & Cabrera S.D. (2002). Late Cretaceous (Campanian) carbon isotope events, sea-level change and correlation of the Tethyan and Boreal realms. *Palaeogeography, Palaeoclimatology, Palaeoecology*, 188: 215-248.
- Jenkyns H.C. (1980). Cretaceous anoxic events: From continents to oceans. *Journal of the Geological Society of London*, 137: 171-188.
- Jenkyns H.C. (1985). The Early Toarcian and Cenomanian–Turonian anoxic events in Europe: Comparisons and contrasts. *Geologische Rundschau*, 74: 505-518.
- Jenkyns H.C. (1988). The Early Toarcian (Jurassic) anoxic event: stratigraphic, sedimentary, and geochemical evidence. *The American Journal of Science*, 288: 101-151.
- Jenkyns H.C. (2010). Geochemistry of oceanic anoxic events. *Geochemistry, Geophysics, Geosystems*, 11: Q03004.
- Jenkyns H.C. & Clayton C.C. (1986). Black shales and carbon isotopes in pelagic sediments from the Tethyan Lower Jurassic. *Sedimentology*, 33: 87-106.
- Jenkyns H.C., Dickson A.J., Ruhl M. & Van den Boom S.H. (2017). Basalt-seawater interaction, the Plenius Cold Event, enhanced weathering and geochemical change: deconstructing Oceanic Anoxic Event 2 (Cenomanian–Turonian, Late Cretaceous). *Sedimentology*, 64: 16-43.
- Jenkyns H.C., Gale A.S. & Corfield R.M. (1994). Carbon- and oxygen-isotope stratigraphy of the English Chalk and Italian Scaglia and its palaeoclimatic significance. *Geological Magazine*, 131: 1-34.
- Jenkyns H.C., Gröcke D.R. & Hesselbo S.P. (2001). Nitrogen isotope evidence for water mass denitrification during the early Toarcian (Jurassic) oceanic anoxic event. *Paleoceanography*, 16: 593-603.
- Jenkyns H.C., Matthews A., Tsikos H. & Erel Y. (2007). Nitrate reduction, sulfate reduction, and sedimentary iron isotope evolution during the Cenomanian–Turonian oceanic anoxic event. *Paleoceanography*, 22: PA3208.
- Kálin O. & Bernoulli D. (1984). *Schizosphaerella* Deflandre and Dangeard in Jurassic deeper-water carbonate sediments, Mazagan Continental Margin (Hole 547b) and Mesozoic Tethys. In Hinz K., Winterer E.L. et al., *Initial Reports of the Deep-Sea Drilling Project*, 79: U.S. Government Printing Office, Washington, 79: 411-435.
- Kamptner E. (1931). *Nannoconus steinmanni* nov. gen., nov. spec., ein merkwürdiges gesteinsbildendes Mikrofossil aus dem jüngeren Mesozoikum der Alpen. *Paläontologische Zeitschrift*, 13: 288-298.
- Keller C.E., Hochuli P.A., Weissert H., Bernasconi S.M., Giorgioni M. & Garcia T.I. (2011). A volcanically induced climate warming and floral change preceded the onset of OAE1a (Early Cretaceous). *Palaeogeography, Palaeoclimatology, Palaeoecology*, 305: 43-49.
- Kuroda J., Ogawa N.O., Tanimizu M., Coffin M., Tokuyama H., Kitazato H. & Ohkouchi N. (2007). Contemporaneous massive subaerial volcanism and late Cretaceous Oceanic Anoxic Event 2. *Earth and Planetary Science Letters*, 256: 211-223.
- Leckie R.M., Bralower T.J. & Cashman R. (2002). Oceanic anoxic events and plankton evolution: Biotic response to tectonic forcing during the mid-Cretaceous. *Paleoceanography*, 17: PA000623.
- Lees J.A., Bown P.R., & Mattioli E. (2005). Problems with proxies? Cautionary tales of calcareous nannofossil paleoenvironmental indicators. *Micropaleontology*, 51: 333-343.
- Lignum J., Jarvis I. & Pearce M. (2007). The dinoflagellate cyst record of the Cenomanian–Turonian boundary (OAE 2): Data from a newly cored black shale succession, Wunstorf, northern Germany. *Geophysical Research Abstracts*, 9: 3854.
- Lini A., Weissert H. & Erba E. (1992). The Valanginian carbon isotope event: a first episode of greenhouse climate conditions during the Cretaceous. *Terra Nova*: 4: 374-384.
- Linnert C., Mutterlose J. & Erbacher J. (2010). Calcareous nannofossils of the Cenomanian/Turonian boundary interval from the Boreal Realm (Wunstorf, northwest Germany). *Marine Micropaleontology*, 74: 38-58.
- Linnert C., Mutterlose J., & Mortimore R. (2011). Calcareous nannofossils from Eastbourne (southeastern England) and the paleoceanography of the Cenomanian–Turonian boundary interval. *Palaios*, 26: 298-313.
- Lohmann H. (1902). Die Coccolithophoridae, eine Monographie der Coccolithen bildenden Flagellaten, zugleich ein Beitrag zur Kenntnis des Mittelmeerauftriebs. *Archiv für Protistenkunde*, 1: 89-165.
- Luciani V., Cobianchi M. & Jenkyns H.C. (2001). Biotic and geochemical response to anoxic events: the Aptian pelagic succession of the Gargano Promontory (southern Italy). *Geological Magazine*, 138: 277-298.
- Malinverno A., Erba E. & Herbert T.D. (2010). Orbital tuning as an inverse problem: Chronology of the early Aptian oceanic anoxic event 1a (Selli Level) in the Cismonte APTICORE. *Paleoceanography*, 25: PA2203.
- Malinverno A., Hildebrandt J., Tominaga M. & Channell J.E.T. (2012). M-sequence geomagnetic polarity time scale (MHTC12) that steadies global spreading rates and incorporates astrochronology constraints. *Journal of Geophysical Research*, 117: B06104.
- Mattioli E. (1997). Nannoplankton productivity and diagenesis in the rhythmically bedded Toarcian–Aalenian Fiuminata section (Umbria–Marche Apennine, central Italy). *Palaeogeography, Palaeoclimatology, Palaeoecology*, 130: 113-133.
- Mattioli E. & Pittet B. (2002). The contribution of calcareous nannoplankton to the carbonate production in the Early Jurassic. *Marine Micropaleontology*, 45: 175-190.
- Mattioli E. & Pittet B. (2004). Spatial and temporal distribution of calcareous nannofossils along a proximal–distal transect in the Umbria–Marche basin (Lower Jurassic; Italy). *Palaeogeography, Palaeoclimatology, Palaeoecology*, 205: 295-316.
- Mattioli E., Pittet B., Bucefalo Palliani R., Röhl H.J., Schmid-Röhl A. & Moretini E. (2004b). Phytoplankton evidence for the timing and correlation of palaeoceanographical changes during the early Toarcian oceanic anoxic event (Early Jurassic). *Journal of the Geological Society*, 161: 685-693.
- Mattioli E., Pittet B., Petitpierre L. & Mailliot S. (2009). Dramatic decrease of pelagic carbonate production by nannoplankton across the early Toarcian anoxic event (T-OAE). *Global Planetary Change*, 65: 134-145.
- Mattioli E., Pittet B., Riquier L. & Grossi V. (2014). The mid-Valanginian Weissert Event as recorded by calcareous nannoplankton in the Vocontian Basin. *Palaeogeography, Palaeoclimatology, Palaeoecology*, 414: 472-485.
- Mattioli E., Pittet B., Suan G. & Mailliot S. (2008). Calcareous nannoplankton changes across the early Toarcian oceanic anoxic event in the western Tethys. *Paleoceanography and Palaeoclimatology*, 23: PA3208.
- Mattioli E., Pittet B., Young J.R. & Bown P.R. (2004a). Biometric analysis of Pliensbachian–Toarcian (Lower Jurassic) coccoliths of the family Biscutaceae: Intra- and interspecific variability versus palaeoenvironmental influence. *Marine Micropaleontology*, 52: 5-27.

- Méhay S., Keller C.E., Bernasconi S.M., Weissert H., Erba E., Bottini C. & Hochuli P.A. (2009). A volcanic CO₂ pulse triggered the Cretaceous Oceanic Anoxic Event 1a and a biocalcification crisis: *Geology*, 37: 819-822.
- Melinte M. & Mutterlose J. (2001). A Valanginian (Early Cretaceous) 'boreal nannoplankton excursion' in sections from Romania. *Marine Micropaleontology*, 43: 1-25.
- Menegatti A.P., Weissert H., Brown R.S., Tyson R.V., Farrimond P., Strasser A. & Caron M. (1998). High resolution δ¹³C stratigraphy through the early Aptian "Livello Selli" of the Alpine Tethys. *Paleoceanography*, 13: 530-545.
- Moretini E., Santantonio M., Bartolini A., Cecca F., Baumgartner P.O. & Hunziker, J.C. (2002). Carbon isotope stratigraphy and carbonate production during the Early-Middle Jurassic: examples from the Umbria-Marche-Sabina Apennines (central Italy). *Palaeogeography, Palaeoclimatology, Palaeoecology*, 184: 251-273.
- Mort H., Jacquat O., Adatte T., Steinmann P., Föllmi K., Matera V., Berner Z. & Stüben D. (2007). The Cenomanian/Turonian anoxic event at the Bonarelli level in Italy and Spain: enhanced productivity and/or better preservation? *Cretaceous Research*, 28: 597-612.
- Nederbragt A.J. & Fiorentino A. (1999). Stratigraphy and palaeoceanography of the Cenomanian-Turonian boundary event in Oued Mellegue, north-western Tunisia. *Cretaceous Research*, 20: 47-62.
- Noël D. & Busson G. (1990). L'importance des schizosphères, stomiosphères, Conusphaera et Nannoconus dans la genèse des calcaires fins pélagiques du Jurassique et du Crétacé inférieur/ Importance of schizospheres, stomiospheres, Conusphaera and Nannoconus in the genesis of Jurassic and Early Cretaceous fine-grained pelagic limestones. *Sciences Géologiques, Bulletin*, 43: 63-93.
- Perch-Nielsen K. (1988). New Lower Cretaceous calcareous nanofossil species from England. *Newsletter of the International Nannoplankton Association*, 10: 30-37.
- Peti L., Thibault N., Clémence M.E., Korte C., Dommergues J.L., Bougeault C., Pellenard P., Jelby M.E. & Ullmann C.V. (2017). Sinemurian–Pliensbachian calcareous nanofossil biostratigraphy and organic carbon isotope stratigraphy in the Paris Basin: Calibration to the ammonite biozonation of NW Europe. *Palaeogeography, Palaeoclimatology, Palaeoecology*, 468: 142-161.
- Premoli Silva I., Erba E., Salvini G., Verga D. & Locatelli C. (1999). Biotic changes in Cretaceous anoxic events. *Journal of Foraminiferal Research*, 29: 352-370.
- Premoli Silva I., Erba E. & Tornaghi M.E. (1989). Palaeoenvironmental signals and changes in surface fertility in mid Cretaceous Corg-rich pelagic facies of the Fucoid Marls (central Italy). *Geobios*, 22: 225-236.
- Renard M. (1986). Pelagic carbonate chemostratigraphy (Sr, Mg, ¹⁸O, ¹³C). *Marine Micropaleontology*, 10: 117-164.
- Reolid M., Mattioli E., Nieto L.M. & Rodríguez-Tovar F. (2014). The Early Toarcian oceanic anoxic event in the external subbetic (Southiberian Palaeomargin, Westernmost Tethys): geochemistry, nanofossils and ichnology. *Palaeogeography, Palaeoclimatology, Palaeoecology*, 411: 79-94.
- Robinson S.A., Heimhofer U., Hesselbo S.P. & Petrizzo M.R. (2017). Mesozoic climates and oceans – a tribute to Hugh Jenkyns and Helmut Weissert. *Sedimentology*, 64: 1-15.
- Sabatino N., Neri R., Bellanca A., Jenkyns H.C., Baudin F., Parisi G. & Masetti D. (2009). Carbon-isotope records of the Early Jurassic (Toarcian) oceanic anoxic event from the Valdorbica (Umbria–Marche Apennines) and Monte Mangart (Julian Alps) sections: palaeoceanographic and stratigraphic implications. *Sedimentology*, 56: 1307-1328.
- Schindelin J., Arganda-Carreras I., Frise E., Kaynig V., Longair M., Pietzsch T., Preibisch S., Rueden C., Saalfeld S., Schmid B., Tinevez J.Y., White D.J., Hartenstein V., Eliceiri K., Tomancak P. & Cardona A. (2012). Fiji: an open-source platform for biological-image analysis. *Nature Methods*, 9: 676.
- Schlanger S.O. & Jenkyns H.C. (1976). Cretaceous oceanic anoxic events: Causes and consequences. *Geologie en Mijnbouw*, 55: 179-184.
- Scholle P.A. & Arthur M.A. (1980). Carbon isotope fluctuations in Cretaceous pelagic limestones: potential stratigraphic and petroleum exploration tool. *American Association of Petroleum Geologists Bulletin*, 64: 67-87.
- Scopelliti G., Bellanca A., Coccioni R., Luciani V., Neri R., Baudin F., Chiari M. & Marcucci M. (2004). High-resolution geochemical and biotic records of the Tethyan 'Bonarelli Level' (OAE2, latest Cenomanian) from the Calabianca–Guidaloca composite section, northwestern Sicily, Italy. *Palaeogeography, Palaeoclimatology, Palaeoecology*, 208: 293-317.
- Scopelliti G., Bellanca A., Erba E., Jenkyns H.C., Neri R., Tamagnini P., Luciani V. & Masetti D. (2008). Cenomanian–Turonian carbonate and organic-carbon isotope records, biostratigraphy and provenance of a key section in NE Sicily, Italy: Palaeoceanographic and palaeogeographic implications. *Palaeogeography, Palaeoclimatology, Palaeoecology*, 265: 59-77.
- Scotese C.R. (ed.) (2014). Atlas of Plate Tectonic Reconstructions (Mollweide Projection), Volumes 1-6, *PALEOMAP Project PaleoAtlas for ArcGIS*, PALEOMAP Project, Evanston, IL.
- Snow L.J., Duncan R.A. & Bralower T.J. (2005). Trace element abundances in the Rock Canyon Anticline, Pueblo, Colorado, marine sedimentary section and their relationship to Caribbean plateau construction and oxygen anoxic event 2. *Palaeogeography*, 20: PA3005.
- Sprovieri M., Coccioni R., Lirer F., Pelosi N. & Lozar F. (2006). Orbital tuning of a lower Cretaceous composite record (Maiolica Formation, central Italy). *Palaeoceanography*, 21: PA4212.
- Sprovieri M., Sabatino N., Pelosi N., Batenburg S.J., Coccioni R., Iavarone M. & Mazzola S. (2013). Late Cretaceous orbitally-paced carbon isotope stratigraphy from the Bottaccione Gorge (Italy). *Palaeogeography, Palaeoclimatology, Palaeoecology*, 379-380: 81-94.
- Stein M., Föllmi K.B., Westermann S., Godet A., Adatte T., Matera V., Fleitmann D. & Berner Z. (2011). Progressive palaeoenvironmental change during the Late Barremian–Early Aptian as prelude to Oceanic Anoxic Event 1a: Evidence from the Gorgo a Cerbara section (Umbria-Marche basin, central Italy). *Palaeogeography, Palaeoclimatology, Palaeoecology*, 302: 396-406.
- Stoll H.M. & Schrag D.P. (2000). High-resolution stable isotope records from the Upper Cretaceous rocks of Italy and Spain: glacial episodes in a greenhouse planet? *Geological Society of America Bulletin*, 112: 308-319.
- Stradner H. (1962). Über neue und wenig bekannte Nanofossilien aus Kreide und Alttertiär. *Sonderabdruck aus den Verhandlungen der Geologischen Bundesanstalt*, 2: 363-377.
- Suan G., Mattioli E., Pittet B., Lecuyer C., Sucheras-Marx B., Duarte L.V., Philippe M., Reggiani L. & Martineau F. (2010). Secular environmental precursors to Early Toarcian (Jurassic) extreme climate changes. *Earth and Planetary Science Letters*, 290: 448-458.
- Suan G., Mattioli E., Pittet B., Maillot S. & Lécuyer C. (2008). Evidence for major environmental perturbation prior to and during the Toarcian (Early Jurassic) oceanic anoxic event from the Lusitanian Basin, Portugal. *Paleoceanography* 23: PA1202.
- Tejada M.L.G., Katsuhiko S., Kuroda J., Coccioni R., Mahoney J.J., Ohkouchi N., Sakamoto T. & Tatsumi Y. (2009). Ontong Java Plateau eruption as a trigger for the early Aptian oceanic anoxic event. *Geology*, 37: 855-858.
- Tremolada F. & Erba E. (2002). Morphometric analysis of the Aptian *Rucinolithus terebrodentarius* and *Assipetra infracretacea* nannoliths: Implications for taxonomy, biostratigraphy and Palaeoceanography. *Marine Micropaleontology*, 44: 77-92.

- Tremolada F., Van de Schootbrugge B. & Erba E. (2005). Early Jurassic schizosphaerellid crisis in Cantabria, Spain: implications for calcification rates and phytoplankton evolution across the Toarcian oceanic anoxic event. *Paleoceanography*, 20: PA2011.
- Tsikos H., Jenkyns H.C., Walsworth-Bell B., Petrizzo M.R., Forster A., Kolonic S., Erba E., Premoli Silva I., Baas M., Wagner T. & Sinninghe Damsté J.S. (2004). Carbon-isotope stratigraphy recorded by the Cenomanian–Turonian Oceanic Anoxic Event: correlation and implications based on three key localities. *Journal of the Geological Society*, London, 161: 711-719.
- van Breugel Y., Schouten S., Tsikos H., Erba E., Price G.D. & Sinninghe Damsté J.S. (2007). Synchronous negative carbon isotope shifts in marine and terrestrial biomarkers at the onset of the early Aptian oceanic anoxic event 1a: Evidence for the release of ^{13}C -depleted carbon into the atmosphere. *Paleoceanography*, 22: PA1210.
- Van de Schootbrugge B., Bailey T.R., Rosenthal Y., Katz M.E., Wright J.D., Miller K.G., Feist-Burkhardt S. & Falkowski P.G. (2005). Early Jurassic climate change and the radiation of organic-walled phytoplankton in the Tethys Ocean. *Paleobiology*, 31: 73-97.
- Voigt S., Aurag A., Leis F. & Kaplan U. (2007). Late Cenomanian to Middle Turonian high-resolution carbon isotope stratigraphy: New data from the Münsterland Cretaceous Basin, Germany. *Earth and Planetary Science Letters*, 253: 196-210.
- Weissert H. (1989). C-isotope stratigraphy, a monitor of paleoenvironmental change: a case study from the Early Cretaceous. *Surveys in Geophysics*, 10: 1-61.
- Weissert H. & Erba E. (2004). Volcanism, CO_2 and palaeoclimate: a Late Jurassic–Early Cretaceous carbon and oxygen isotope record. *Journal of the Geological Society*, 161: 695-702.
- Weissert H., Lini A., Föllmi K.B. & Kuhn O. (1998). Correlation of Early Cretaceous carbon isotope stratigraphy and platform drowning events: a possible link? *Palaeogeography, Palaeoclimatology, Palaeoecology*, 137: 189-203.
- Weissert H., McKenzie J.A. & Channell J.E.T. (1985). Natural variations in the carbon cycle during the Early Cretaceous. In Sundquist E.T. & Broecker W.S. (eds), *The Carbon Cycle and Atmospheric CO_2 : Natural variations Archean to the Present. Geophysical Monographs*, 32: 531-545.
- Wiegand G.E. (1984). Two New Genera of Calcareous Nannofossils from the Lower Jurassic. *Journal of Paleontology*, 58: 1151-1155.

Manuscript received 20 March 2019

Revised manuscript accepted 2 April 2019

Published online 30 April 2019

Guest Editors Massimo Bernardi & Giorgio Carnevale